Performance Evaluation and Chemical Characterization of Asphalt Binders and Mixtures Containing Recycled Polyethylene

A Final Report

Submitted to

Patrick Krieger
Plastics Industry Association

By

Fan Yin
Raquel Moraes
Mawazo Fortunatus
Nam Tran
National Center for Asphalt Technology

and

Michael D. Elwardany
Jean-Pascal Planche
Western Research Institute

March 10, 2020

TABLE OF CONTENTS

ACKNOWLEDGEMENTS

The authors would like to acknowledge the Plastics Industry Association (PLASTICS) for providing the financial support for this research study. The authors would also like to thank the PLASTICS New End Market Opportunities (NEMO) Asphalt Workgroup for providing guidance and feedback to the study. Finally, acknowledgement goes to Adam Taylor, Pamela Turner, Vickie Adams, Tina Taylor, Macabe Faulkner, and Matthew Kmetz at the National Center for Asphalt Technology, Pamela J. Coles, Zackari Hunter, and Nicholas D. Boltonat at the Western Research Institute, and Kevin Cronin at the Ultra-Poly Corporation for their assistance with the laboratory-related activities.

DISCLAIMER

The contents of this report reflect the views of the authors who are responsible for the accuracy of the data and analysis presented herein. The contents do not necessarily reflect the official views or policies of the Plastics Industry Association, the National Center for Asphalt Technology, Auburn University, or the Western Research Institute. This report does not constitute a standard, specification, or regulation. Comments contained in this paper related to specific testing equipment and materials should not be considered an endorsement of any commercial product or service; no such endorsement is intended or implied**.**

1. INTRODUCTION

The asphalt pavement industry has a history of using polymer modification to improve the performance of asphalt binders and extend the service life of asphalt pavements. Many polymers can be used to formulate polymer modified asphalt (PMA) binders, but only a few can provide specified performance at a competitive cost. In general, polymers used for asphalt modification can be classified into thermoplastic plastomers, such as polyethylene (PE) and ethylene vinyl acetate (EVA), elastomers, such as styrene-butadiene rubber (SBR), and thermoplastic elastomers, such as styrene-butadiene-styrene (SBS). Recently, the use of recycled plastics in asphalt mixtures has triggered the interest of both the plastics and asphalt pavement industries. This recycling effort can provide substantial environmental benefits because these recycled materials would otherwise be landfilled, burned, or discarded in the natural environment as trash and litter. According to the Environmental Protection Agency (*2018*), approximately 33 million tons of plastics were generated in 2014, with only less than 10 percent being recycled. Among the plastics generated, linear low-density polyethylene (LLDPE), low-density polyethylene (LDPE), and high-density polyethylene (HDPE) combined account for the largest proportion of over 35 percent. These plastics fall within the category of commodity thermoplastics. Commodity thermoplastics can be re-softened to their original condition by heat, allowing them to be recycled. Additional thermoplastics include acrylonitrile-butadiene-styrene (ABS), polyethylene terephthalate (PET), polypropylene (PP), polystyrene (PS), and polyvinyl chloride (PVC) (*ACC, 2019*).

There are two approaches of incorporating recycled plastics in asphalt pavements: the wet process and the dry process (*NCAT, 2019*). In the wet process, recycled plastics are added to the asphalt binder as polymer modifiers, where mechanical mixing is required to achieve a homogenous modified binder blend. In the dry process, recycled plastics are added directly to the mixture as aggregate replacement or mixture modifiers. The main obstacle to the implementation of the dry process is a concern of lack of consistency of the final produced mix. However, the wet process also has limitations due to the poor storage stability of the plastic modified binders, where the recycled polymers tend to separate from the asphalt binder due to the difference in density and viscosity as well as the incompatibility between the two components.

India reportedly has over 15 years of experience recycling waste plastics in asphalt pavements using the dry process. The Indian Roads Congress (IRC) specification (*2013*) allows the incorporation of up to 10 percent of LDPE, HDPE, polyurethane, and PET by weight of asphalt binder. During mix production, waste plastic materials are added to the aggregates at an elevated temperature of 160 to 180°C, where the plastics are melted and coat the surface of the aggregates. Existing studies indicate that aggregate particles coated with waste plastics have enhanced toughness, abrasion resistance, bond strength, and reduced asphalt absorption, which consequently yield asphalt mixtures with better resistance to rutting, fatigue damage, and moisture susceptibility (*CPCB, 2008; Bajpai et al., 2017*).

Over the last few years, several test sections have been constructed in Europe using a series of proprietary recycled plastic products (*MacRebur, 2019*). White and Reid (*2018*) reported that these plastic products improved mixture stiffness, rutting resistance, and fracture toughness

while reducing the amount of asphalt binder required in the mixture by approximately 6 to 10 percent. Nonetheless, their impact on the performance of asphalt pavements remains unknown and warrants further investigation.

In February 2019, Dow completed two private road projects in Texas using asphalt binders modified with recycled plastics following the wet process (*Brown et al., 2019*). The binder formulation used was a neat performance grade (PG) 64-22 binder modified with 1.5% LLDPE-rich post-consumer plastics, ELVALOY™ reactive elastomeric terpolymer (RET), and polyphosphoric acid (PPA). The final modified binder met the Texas Department of Transportation's PG 70-22 specifications.

Over the last decade, several laboratory studies in Asia and Africa have reported successful experience using recycled plastics [mainly recycled polyethylene (RPE)] for asphalt modification. These studies found that adding RPE significantly increased the stiffness and rutting resistance of asphalt binders and mixtures, and thus, had the potential to improve the performance of asphalt pavements and extend their service lives (*Ho et al., 2006; Liao et al., 2006; Yang and Liu, 2010; Gawande et al., 2012; Silva et al., 2013; Appiah et al., 2017*). However, it should be noted that in most of the Asian and African countries, rutting is the primary form of distress for asphalt pavements, while in the United States, rutting problems have been virtually eliminated. Instead, state and local highway agencies are facing the challenge of premature cracking and durability issues of asphalt pavements due to the limitations of the Superpave mix design system, increased use of recycled asphalt materials [i.e., reclaimed asphalt pavement (RAP) and recycled asphalt shingles (RAS)], and declining quality of the asphalt binders, among other factors (*West et al., 2018; Tran et al., 2019; Planche et al., 2018; Elwardany et al., 2019; Adams et al., 2019*). Therefore, research is needed to establish a better understanding of the impact of recycled plastics on the performance, especially durability and cracking resistance, of asphalt binders and mixtures.

2. OBJECTIVES

The objective of this study was twofold:

- Firstly, to characterize the chemical and rheological properties of asphalt binders modified with RPE and reactive elastomeric terpolymers (RET) as compatibilizers and performance-enhancing additives.
- Secondly, to determine the impact of using both RPE and RPE plus RET for asphalt modification on the rutting, cracking, and moisture resistance of asphalt mixtures.

3. EXPERIMENTAL DESIGN

Figure 1 illustrates the experimental design of the study. A total of nine RPE modified binders were prepared using one neat performance graded (PG) 58-28 binder, one RPE sample, and two RET additives (referred to as RET1 and RET2) along with PPA as a catalyst. Four of the RPE modified binders were prepared by modifying the neat binder with different RPE dosages, ranging from 2% to 5%, and the other five binders were prepared by modifying the neat binder with a combination of RPE and RET. The nine modified binders were first tested to determine their storage stability, and those passing the Georgia Department of Transportation (GDOT)

requirement (based on softening point test) were further evaluated in three complementary experiments.

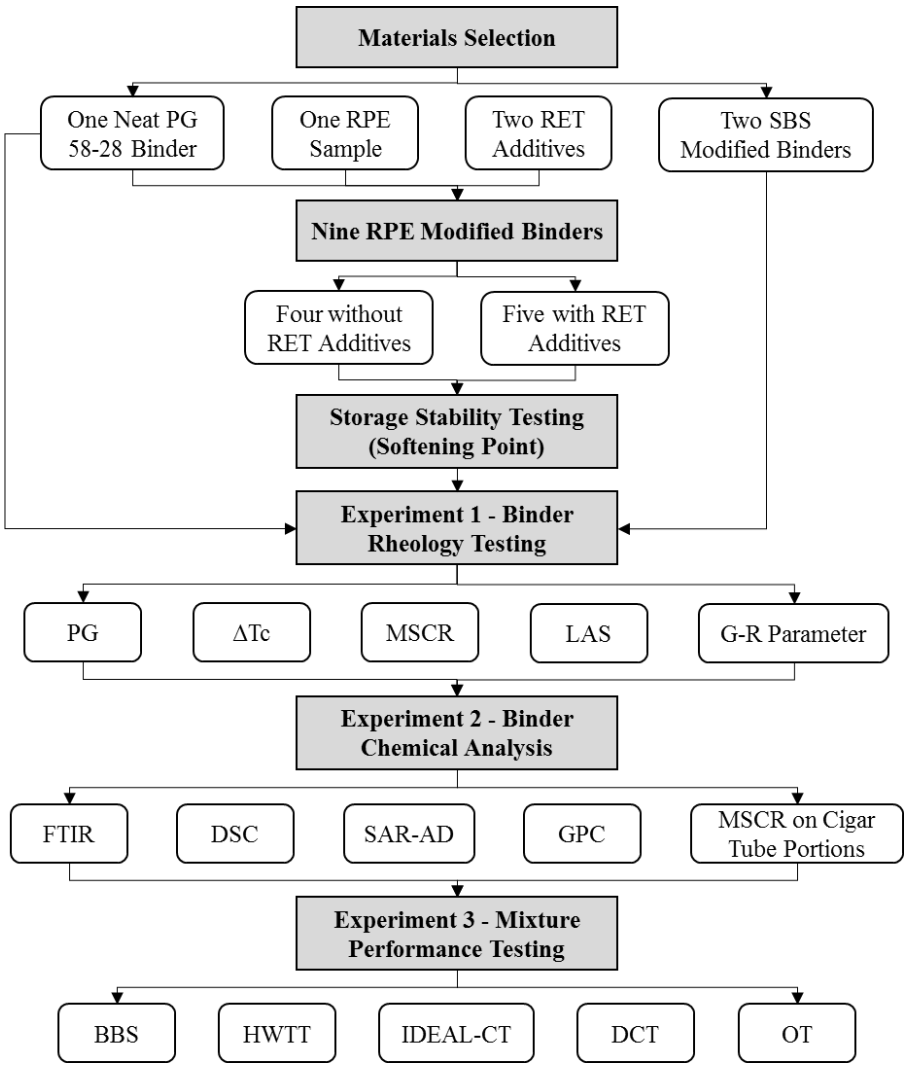

Figure 1. Experimental Design of the Study

The first experiment focused on binder rheological evaluation, where several asphalt binder rheological tests and parameters were used, including performance grading (PG), delta T_c (ΔT_c), multiple stress creep recovery (MSCR), linear amplitude sweep (LAS), and Glover-Rowe (G-R) parameter. For performance comparison, the neat PG 58-28 binder and two SBS modified binders, with similar PG and delta Tc (ΔT_c) as the RPE and RPE+RET modified binders, were also tested. The goal of this experiment was to determine the effect of RPE and RET on the rheological properties of asphalt binders.

The second experiment focused on binder chemical evaluation, where four selected asphalt binders (i.e., neat, RPE modified, RET modified, and RPE+RET modified) were characterized using Fourier-transform infrared spectroscopy (FTIR), differential scanning calorimetry (DSC), saturate, aromatic, resin, and asphaltenes determinator (SAR-AD), and gel

permeation chromatography (GPC). Additionally, a modified storage stability test based on MSCR testing of cigar tube portions was conducted.

Finally, the last experiment focused on mixture performance testing. Binder bond strength (BBS), Hamburg wheel tracking test (HWTT), indirect tensile cracking test (IDEAL-CT), disc-shaped compact tension (DCT) test, and Texas overlay test (OT) were conducted to determine the impact of adding RPE and RPE plus RET on the performance properties of asphalt mixtures.

3.1 Materials Selection

The neat PG 58-28 binder used for RPE modification in the study was from Alberta, Canada. The RPE sample used was supplied by EREMA North America, Inc. Thermogravimetry and differential scanning calorimetry testing on the RPE sample indicated that it had a specific gravity of 0.939, an ash content of 7.1%, a melting temperature of 120°C, and a polymer resin makeup of 94% LDPE and 6% HDPE combined (*Cronin, 2019*).

Two ethylene-based RET additives were used as compatibilizers to mitigate the polymer separation of RPE modified binders. When added in the asphalt binder, the RET additives were expected to act as a steric stabilizer, hindering the coalescence of RPE particles. Additionally, the elastomeric nature of the RET additives would yield the resultant modified binders with enhanced fatigue tolerance and overall flexibility, providing performance benefits (*Panabaker, 2007*). Finally, two SBS modified binders were included; one was formulated with 2.4% linear SBS polymer and had a PG of 64-28, and the other contained 4.2% linear SBS polymer and had a PG of 70-28.

For mixture performance testing, a 9.5mm nominal maximum aggregate size (NMAS) Superpave mix containing 20 percent RAP was used. The mix had a volumetric optimum binder content of 5.5 percent with 4.0 percent air voids and 15.6 percent voids in mineral aggregate (VMA) at 80 design gyrations. The RAP binder replacement was approximately 18 percent. The same mix design was followed to prepare performance test specimens for asphalt mixtures containing the neat, RPE modified, RPE+RET modified, and SBS modified binders.

3.2 Preparation of RPE Modified Binders and Mixtures

To prepare an RPE modified binder, the neat PG 58-28 binder was first preheated in an oven for two hours at 180°C. The RPE sample was then added to the binder and blended for one hour using a high-speed shear mixer [3,000 revolutions per minute (rpm)]. In cases where a RET additive was used, the RPE modified binder was then transferred to a low-speed shear mixer (200 rpm) and blended for 10 minutes at 180°C. Finally, the RET additive and a catalyst (i.e., PPA) were added to the binder and blended for one to two hours until a homogeneous binder blend was achieved, as shown in Figure 2.

(a) (b) (c)

Figure 2. Laboratory Preparation of RPE and RPE+RET Modified Blends at WRI; (a) High-shear Mixer Setup, (b) High-shear Mixing of RPE Samples, and (c) Low-shear Mixing of RET Additive

For the preparation of mixture performance test specimens, asphalt binders and RAP were preheated in an oven for two to three hours at a specified mixing temperature (Table 1) and 275°F, respectively. The virgin aggregates were preheated overnight at 360°F. For RPE and RPE+RET modified mixtures, a low-speed shear mixer (200 rpm) was set up adjacent to the planetary mixer, which was used to blend the modified binder for 15 minutes at an elevated temperature (10 to 15°F above mixing temperature) prior to being mixed with the aggregates and RAP. The intention of this additional blending process was to prevent the phase separation of RPE or RPE+RET modified binder and ensure that a homogenous binder blend was used for mixing. After mixing, the loose mix was conditioned in an oven for four hours at 275°F. In this study, HWTT specimens were compacted upon completion of this four-hour conditioning process. For DCT specimens, the loose mix was further aged in an oven for six hours at 275°F while eight hours of long-term aging was used for the IDEAL-CT and OT specimens. Note that these two long-term aging protocols were expected to simulate approximately three to five years of field aging in asphalt pavements in most of the continental U.S. All performance specimens were tested within two weeks after being prepared.

Table 1. Mixing and Compaction Temperature for Asphalt Binders Used in the Study

Binder ID	Mixing Temperature	Compaction Temperature
58-28 (Neat)	305°F	275°F
64-28 (58-28+3%RPE)	320°F	295°F
70-28 (58-28+3%RPE+RET1)	325°F	310°F
70-28 (4.2% SBS)	325°F	310°F

3.3 Laboratory Binder Tests

3.3.1 Storage Stability

The storage stability test was conducted in accordance with ASTM D7173. During the test, a measured quantity of RPE and RPE+RET modified binder was placed in a sealed aluminum tube and then conditioned in a vertical position for 48 hours at 163°C. After the static heat conditioning, the binder was submitted to a freezing cycle for four hours at -10°C. Then, the top and bottom portions of the binder were separated (Figure 3) and tested to determine the softening point using the ring-and-ball apparatus per ASTM D36. Approval of storage stability test

results was made following the GDOT specification (*2013*), which requires a maximum allowable difference of 10°C in the softening point between the top and bottom binder samples. Additionally, a modified test procedure based on MSCR testing of top versus bottom cigar tube portions was evaluated on selected RPE and RPE+RET modified binders at WRI. The MSCR test procedure will be discussed in Section 3.3.3.

Figure 3. Binders Taken Out from the Various Cigar Tube's (top, middle, and bottom) Portions

3.3.2 Superpave Performance Grading (PG) and Delta Tc Parameter

The continuous performance grades of the neat, RPE modified, RPE+RET modified, and SBS modified binders were determined following ASTM D7642. Additionally, the ΔT_c of 20-hour PAV aged binder sample was determined based on the bending beam rheology (BBR) results, where ΔT_c is defined as the numerical difference between the low continuous grade temperatures determined from the BBR stiffness criterion of 300 MPa and the m-value criterion of 0.3 (*Anderson et al., 2011*). The ΔT_c parameter has recently been used to assess the loss of stress relaxation properties of asphalt binders. Generally, a more positive (or less negative) ΔT_c value is desirable for asphalt binders with satisfactory ductility and block cracking resistance; however, its applicability to PMA binders warrants further investigation.

3.3.3 Multiple Stress Creep Recovery (MSCR)

The MSCR test per AASHTO T 350 was used to evaluate the elastic response and rutting resistance of RPE modified binders versus the neat and SBS modified binders. The test was conducted on rolling thin film oven (RTFO)-aged binder residues. The test applied 20 loading cycles at a low stress level of 0.1 kPa followed by 10 cycles at a high stress level of 3.2 kPa. Each loading cycle consisted of 1 second of creep and 9 seconds of recovery. For data analysis, the strain responses were utilized to calculate the percent recovery (%R) and non-recoverable creep compliance (J_{nr}) using Equation 1 and Equation 2, respectively. A higher %R value and a lower J_{nr} value indicate better binder elasticity and rutting resistance, respectively. In this study, the MSCR test was conducted at a constant temperature of 64°C.

$$\%R = \frac{\varepsilon_r}{\varepsilon_r + \varepsilon_{nr}} * 100\% \qquad \text{Equation 1}$$

Where,

ε_r = recoverable strain; and

ε_{nr} = non-recoverable strain.

$$J_{nr} = \frac{\varepsilon_{nr}}{\sigma} \quad \text{Equation 2}$$

Where,

σ = creep stress.

3.3.4 Linear Amplitude Sweep (LAS)

The LAS test per AASHTO TP 101 was utilized to evaluate the fatigue resistance of neat, RPE modified, and SBS modified binders. The test was conducted on pressure aging vessel (PAV)-aged binder residues at the intermediate PG temperature. The test consisted of two procedures: a frequency sweep test and an amplitude sweep test. The binder was first tested in the frequency sweep test to determine its linear viscoelasticity and then tested in the amplitude sweep test, where a series of oscillatory load cycles at systematically increasing amplitudes (up to 30% applied strain) was applied to cause accelerated fatigue damage. For data analysis, the continuum damage theory was used (*Kim et al., 2006; Hintz et al., 2011*). The major outcome of the test was a relationship between the fatigue parameter (N_f, normalized to 1 million ESALs) versus the applied shear strain as a pavement structure indicator (Equation 3). At a certain strain level, asphalt binders with a higher N_f value are expected to have better resistance to fatigue damage.

$$N_f = A_{35}(\gamma_{\max})^{-B} \quad \text{Equation 3}$$

Where,

γ_{max} = the maximum expected binder strain for a given pavement structure; and
A_{35}, B = fatigue performance model parameters.

3.3.5 Glover-Rowe (G-R) Parameter

To determine the G-R parameter, dynamic shear rheometer (DSR) frequency sweep test was conducted at multiple test temperatures over an angular frequency range of 0.1 to 10 rad/s. During the test, the peak-to-peak strain of the binder sample was controlled at one percent to ensure its behavior remained in the linear viscoelastic range. For data analysis, the RHEA software was used to construct a limited DSR master curve by fitting the shear complex modulus ($|G^*|$) and phase angle (δ) data to the discrete relaxation and retardation spectra (*Baumgaertel and Winter, 1989*). Then, the binder $|G^*|$ and δ at 15°C and 0.005 rad/s were determined, from which the G-R parameter was calculated using Equation 4. The G-R parameter considers both binder stiffness and embrittlement and is indicative of binder's ductility and block cracking potential. Neat asphalt binders with G-R parameters over 180 kPa and 600 kPa are considered susceptible to the onset of block cracking and significant cracking, respectively (*Rowe, 2011*). However, caution should be exercised when using these limits thresholds because they were developed based on a limited number of field projects in Pennsylvania and their applicability to polymer modified binders remains unknown.

$$G-R\ Parameter = \frac{|G^*|\cos(\delta)^2}{\sin(\delta)}$$ Equation 4

Where,

$|G^*|$ = binder shear complex modulus at 15°C and 0.005 rad/s; and

δ = binder phase angle at 15°C and 0.005 rad/s.

3.3.6 Fourier-Transform Infrared Spectroscopy (FTIR)

According to Jennings et al. (*1980*), Liu et al. (*1998*), and Petersen (*2009*), the change of chemical structure of asphalt binders can be obtained by the calculation of functional and structural indices of some groups from FTIR spectra, since with oxidative aging the absorbance bands representing oxygen containing functionalities (e.g., ketones, sulfoxides, dicarboxylic anhydrides and carboxylic acids) of asphalt increase. In this study, the asphalt binder samples were heated at 150°C before FTIR-attenuated total reflectance (ATR) testing. After the samples reached a workable viscosity, a thin layer of asphalt binder was applied on top of a single bounce diamond crystal for FTIR-ATR analysis. The scans were taken with a resolution of 4 cm^{-1} and saved as interferograms after 64 scans were performed. To quantify oxidation-related changes collected by means of infrared absorption, band areas rather than peak absorbance values were used. The absorption spectrum carbonyl area (C=O) was calculated by integrating the area of the spectrum between the wavelengths of 1660 and 1753 cm^{-1} and using the magnitude of the absorption at 1753 cm^{-1} as the baseline (*RILEM, 2012*). For asphaltic materials, because of overlapping between the peaks at approximately 1700 cm^{-1} (carbonyl functions) and 1600 cm^{-1} (aromatic function), it has been preferred to consider the surface area between these two limits (*RILEM, 2012*). Both ranges are indicators of binder aging, as they reflect the degree of oxidation. In addition to carbonyl area (C=O), the sulfoxide (S=O) area was calculated by integrating the area of the spectrum between the wavelengths of 995 and 1047 cm^{-1} and using the magnitude of the absorption at 1047 cm^{-1} as the baseline.

3.3.7 Differential Scanning Calorimetry (DSC)

The DSC test was conducted using a DSC Q2000 from TA instruments. The asphalt binder samples were sealed in hermetic aluminum pans with sample weights ranging from 8 to 14 milligrams. Before testing, the binder samples were heated at 165°C for five minutes to remove the thermal history. After the initial sample preparation, the samples were cooled to -90°C at a rate of 5°C/min without modulation and then equilibrated at -90°C for 5 minutes. After that, the samples were heated to 165°C at a rate of 10°C/min. The DSC results were used to determine both the melting and crystallization temperatures from the total heat flow curve. In addition, the amount of crystallizable fraction in the asphalt binder sources was estimated from the total heat flow curve, considering that pure wax has a crystallization energy of 180 J/g (*Turner and Branthaver, 1997; Adams et al., 2019*). The crystallizable fraction has been proposed to relate to the physical hardening and low-temperature cracking behaviors of asphalt binder (*Claudy et al., 1992*). Additional modulated DSC cooling and heating cycles were conducted between -90°C and 165°C at 2°C/min, with ±0.5°C modulation every 80 seconds, for determination of the glass transition temperatures of the asphalt binder samples (*Turner and Branthaver, 1997; Adams et al., 2019*).

3.3.8 Saturate, Aromatic, Resin and Asphaltene Determinator (SAR-AD^{TM}) Fractions

An automated high performance liquid chromatography (HPLC) system combined with WRI's patented automated SAR-AD (Saturates, Aromatics, Resins, and Asphaltene Determinator) separation (SAR-AD), was used to study the relative content of eight asphalt fractions based on solubility and polarity: Saturates, Aromatics-1, Aromatics-2, Aromatics-3, Resins, Cyclohexane-Soluble Asphaltenes, Toluene-Soluble Asphaltenes, and Methylene Chloride-Soluble Asphaltenes (*Boysen and Schabron, 2013; Adams et al., 2019; Elwardany et al., 2019*). The SAR-AD device uses two different detectors to analyze the material which elutes from the various columns; (1) Evaporative lights scattering detector (ELSD) that provides an approximate weight percent of material for each fraction, and (2) an optical absorbance detector set at 500 nm which quantifies the presence of chromophores containing material that absorb visible light at 500 nm wavelength.

3.3.9 Gel Permeation Chromatography (GPC)

GPC was used in this study to determine the molecular size distribution (MSD) of asphalt binders, providing a distinct and reproducible molecular-size distribution curve (chromatogram) of the asphalt binder samples in solution. In this method, the asphalt binder is dissolved in a solvent and then injected into the GPC system. The injected sample travels through a series of columns which separates the sample based on molecular size. The larger molecular size particles exit the columns first and are detected by the system's detectors. The smaller molecular size particles travel into the pores of the columns and, therefore, have longer retention times. As a result, a molecular size distribution (which can be thought of as analogous to a type of sieve analysis of the sample) is obtained. In this study, the asphalt samples were prepared using 3% wt./vol. solutions. The detector used for the GPC analysis was the differential refractometer, which is a concentration sensitive detector that measures the difference in refractive index (dRI) between the solvent in the reference side, and a combination of the sample and solvent in the sample side. The set of two GPC columns used were Phenomenex "Phenogel™": the first was 10µm 10E4Å followed by a 5µm 10E3Å column.

3.4 Laboratory Mixture Tests

3.4.1 Binder Bond Strength (BBS) Test

In this study, the Binder Bond Strength Test (BBS) (AASHTO T361), which is a significantly modified version of the original Pneumatic Adhesion Tensile Testing Instrument (PATTI) developed for the coating industry, was used to evaluate the effect of water (i.e., moisture conditioning) on the bond strength of asphalt-aggregate systems. Moraes et al. *(2011)* investigated the feasibility of the BBS test for bond strength characterization and found that the test is repeatable and reproducible. As shown in Figure 4(a), the BBS device is comprised of a portable pneumatic adhesion tester, pressure hose, piston, reaction plate, and a metal pull-out stub. The pull-off tensile strength (POTS) is calculated in accordance to Equation 5 before and after the immersion of each asphalt-aggregate system in water for 48 hours [Figure 4(b) and Figure 4(c)].

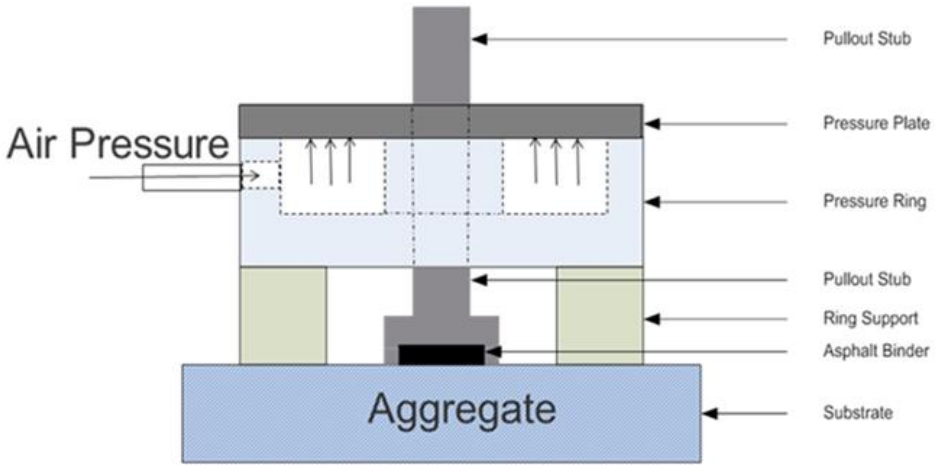

(a)

(b)

(c)

Figure 4. Binder Bond Strength Test; (a) Schematic (*Moraes et al., 2011*), (b) Asphalt-Aggregate System, (c) Moisture Conditioning @ 40°C

$$POTS = \frac{(BP \times Ag) - C}{A_{ps}} \qquad \text{Equation 5}$$

Where,

A_g = Contact Area of Gasket with Reaction Plate (mm^2);
BP = Burst pressure (kPa);
A_{ps} = Area of Pull-off Stub (mm^2); and
C = Piston Constant.

The BBS testing procedure is briefly summarized as follows: (1) before testing, the air supply and pressure hose connection should be checked. Set the rate of loading to 100 psi/sec; (2) place circular spacer under the piston to make sure that the pull-off system is straight and that eccentricity of the stub is minimized; (3) carefully place the piston around the stubs and resting on the spacers not to disturb the stub or to induce unnecessary strain in the sample. Screw the reaction plate into the stub until the pressure plate just touches the piston; (4) apply

pressure at specified rate. After testing, the maximum pull-off tension is recorded, the failure type at the asphalt-aggregate interface is observed, and the surface area exposed is manually interpreted to differentiate the mode of failure (cohesive, adhesive, or combined failure mode) (*Moraes et al., 2011; Rad et al., 2017*) (Figure 5). Note that in this study, the aggregate substrate used was granite aggregate from Junction City, GA and the average pull-off strength was calculated from three replicates.

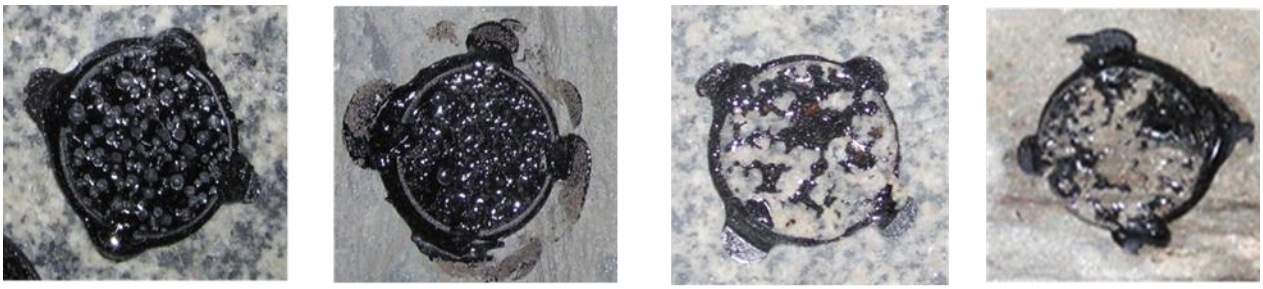

Figure 5. BBS Test Failure Type; (a) Mainly Cohesive Failure, (b) Mainly Adhesive Failure (*Moraes et al., 2011*)

3.4.2 Hamburg Wheel Tracking Test (HWTT)

The HWTT per AASHTO T 324 was utilized to assess the rutting resistance of RPE and RPE+RET modified mixtures versus those containing the neat and SBS modified binders. As shown in Figure 6(a), two sets of HWTT specimens were tested under 158 ± 1 lbs. wheel loads for up to 20,000 passes while submerged in a water bath maintained at a temperature of 50°C. While being tested, rut depths were measured by two linear variable differential transformers (LVDTs), which recorded the relative vertical positions of the load wheels after each load cycle. Two rutting test parameters were used for HWTT data analysis: the corrected rut depth at 20,000 load passes (CRD_{20k}) and rutting resistance index (*RRI*). CRD_{20k} is a simplified version of the viscoplastic strain increment parameter ($\Delta\varepsilon^{vp}$) proposed by Yin et al. (*2014*), which represents the projected rut depth at 20,000 passes solely due to the permanent deformation of the mixture. Figure 6(b) illustrates the determination of CRD_{20k} based on a HWTT rut depth curve. *RRI* was developed by Wen et al. (*2016*) to overcome the difficulty of comparing HWTT results with different test termination points (e.g., results terminated at 20,000 passes versus those terminated at a specified maximum rut depth). As expressed in Equation 6, *RRI* considers both rut depth and the number of wheel pass at completion of the test. A lower CRD_{20k} value but a higher RRI value are desired for asphalt mixtures with better rutting resistance.

$$RRI = N_{\max} * (1 - RD_{\max}) \qquad \text{Equation 6}$$

Where,

N_{max} = number of wheel pass at completion of test; and
RD_{max} = rut depth in inches at completion of test.

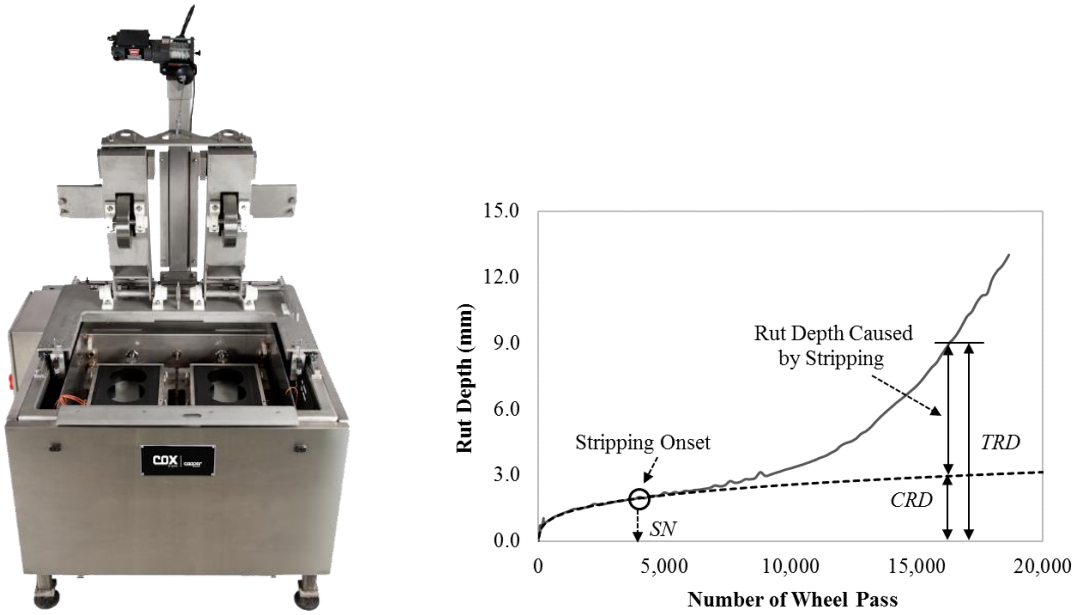

(a) (b)

Figure 6. Hamburg Wheel Tracking Test; (a) Test Device and Specimen Setup, (b) Data Analysis

3.4.3 Indirect Tensile Asphalt Cracking Test (IDEAL-CT)

The IDEAL-CT was used to determine the intermediate-temperature cracking resistance of asphalt mixtures in this study. The test was conducted in accordance with ASTM D8225-19. As shown in Figure 7(a), during the test, a monotonic load was applied along a gyratory specimen at a constant displacement rate of 50 mm/min. The test was performed at 25°C. For data analysis, the load-displacement curve was analyzed to determine the work of fracture, which refers to the total area under the curve, and the slope of the curve at 25 percent reduction from the peak load [Figure 7(b)]. The final test parameter, cracking tolerance index (CT_{index}), was then calculated using Equation 7. A higher CT_{index} value is desired for asphalt mixtures with better cracking resistance.

$$CT_{index} = \frac{t}{62} * \frac{l_{75}}{D} * \frac{G_f}{|m_{75}|} * 10^6 \qquad \text{Equation 7}$$

Where,

t = specimen thickness;
l_{75} = displacement at 75% of peak load;
D = specimen diameter;
G_f = fracture energy; and
$|m_{75}|$ = slope at 75% peak load.

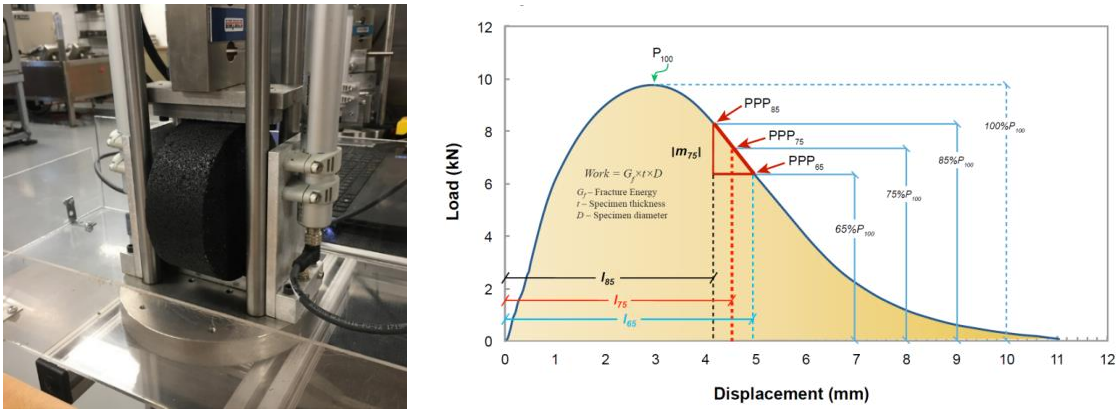

(a) (b)

Figure 7. Indirect Tensile Asphalt Cracking Test; (a) Test Device and Specimen Setup, (b) Data Analysis (*Zhou et al., 2017*)

3.4.4 Disc-shaped Compact Tension (DCT) Test

The DCT test was used to assess the low-temperature fracture resistance of asphalt mixtures containing different types of asphalt binders. The test was conducted in accordance with ASTM D 7313-13. A minimum of four replicate specimens were tested. The final DCT specimen was 50 ± 5 mm thick, which was cut from a larger gyratory sample initially compacted to 160 mm tall and 150 mm in diameter. The specimen was then trimmed to possess a flat edge on one side of the specimen for instrumentation gage points, a 62.5 ± 5.0 mm notch down the center of the specimen from the flat edge, and two 1-inch diameter holes on each side of the notch. The recommended test temperature per ASTM D 7313-13 is the low-temperature PG of the binder plus 10°C. Since all the binders used in the study had a low-temperature PG of -28, the test was conducted at -18°C. Prior to testing, the DCT specimen was loaded in tension by metal rods that were inserted through the specimen core holes, as shown in Figure 8(a). A clip gage was then installed over the crack mouth prior to the start of the test to control and record the crack mouth opening displacement (CMOD). The test was conducted in CMOD control mode with the clip gage opening at a constant rate of 0.017 mm/sec. The test was terminated when the load dropped below 0.1 kN. Figure 8(b) presents an example of the load versus CMOD behavior in the DCT test. For data analysis, the fracture energy (G_f) was calculated using Equation 8, where the area under the load-CMOD curve was determined through numerical integration using the trapezoid rule. A higher G_f value is desired for asphalt mixtures with better resistance to low-temperature cracking.

$$G_f = \frac{Area}{B*(W-a)} \qquad \text{Equation 8}$$

Where,

G_f = fracture energy (J/m^2);
Area = area under load-CMOD curve;
B = specimen thickness (m); and
W-a = initial ligament length (m).

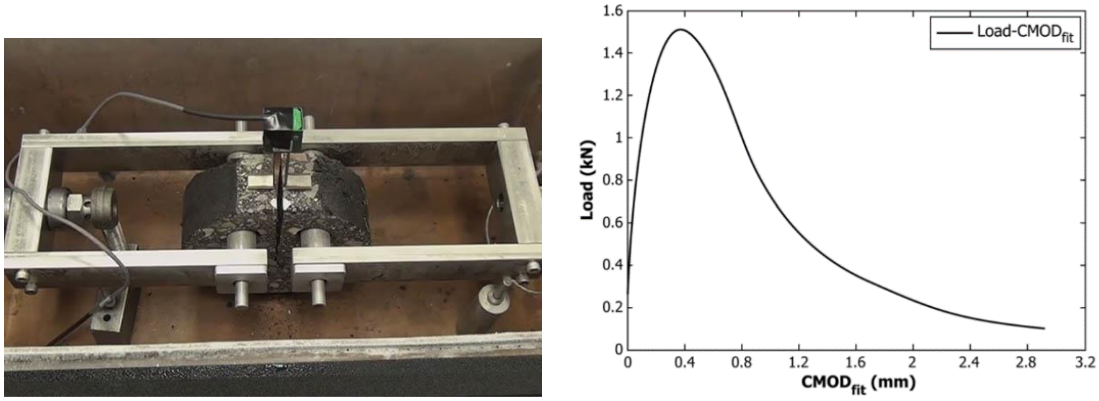

(a) (b)

Figure 8. Disc-shaped Compact Tension Test; (a) Test Device and Specimen Setup, and (b) Load versus CMOD Curve

3.4.5 Texas Overlay Test (OT)

The OT was used to evaluate the reflective cracking resistance of asphalt mixtures in this study. The test was conducted in accordance with Tex-248-F. The OT specimen was cut from a gyratory sample initially compacted to 125mm tall and 150mm in diameter. Prior to testing, the OT specimen was glued to two metal plates with a 4.2mm gap between them and attached to the OT fixture in the Asphalt Mixture Performance Tester (AMPT), as shown in Figure 9(a). During the test, one plate remained fixed while the other plate moved in a displacement control mode while applying a sawtooth wave load to a maximum opening displacement of 0.635 mm once per a 10 second cycle (5 seconds of loading and 5 seconds for unloading). The test was conducted at 25°C. The peak load of each cycle was measured, and the test was terminated when a cycle registered a 93% reduction of the initial peak load. For data analysis, the crack driving force (maximum peak load) data was first plotted to generate a load reduction curve, which was then normalized by the maximum peak load of the first loading cycle [Figure 9(b)]. Finally, a power function was used to fit the normalized load reduction curve and the absolute value of the power coefficient was determined as the final OT parameter, crack progression rate (β). β is indicative of the overall flexibility and fatigue properties of asphalt mixtures during the crack propagation phase. A lower β value (indicating a more moderate normalized load reduction curve) is desired for asphalt mixtures with better resistance to reflective cracking.

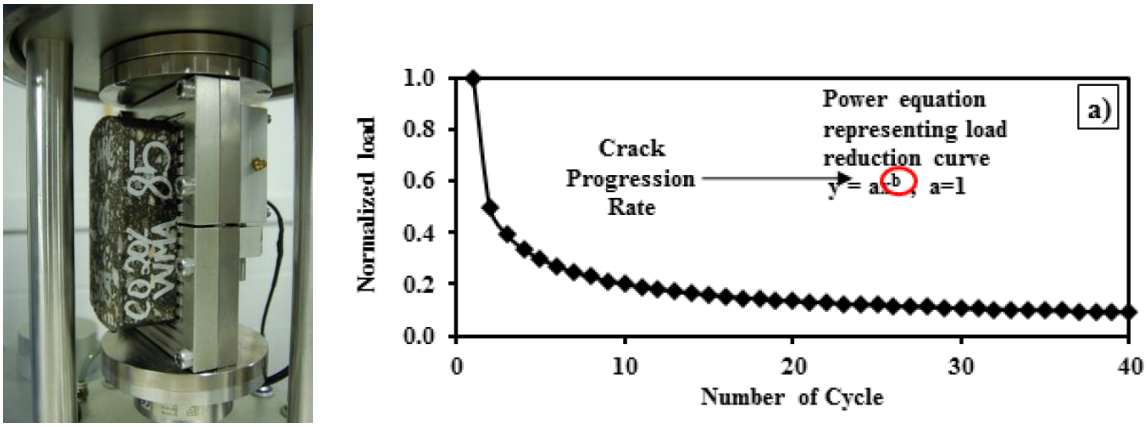

(a) (b)

Figure 9. Texas Overlay Test; (a) Test Device and Specimen Setup, (b) Data Analysis (*Garcia et al., 2017*)

4. BINDER RHEOLOGY TEST RESULTS

4.1 Storage Stability

Table 2 summarizes the storage stability results of the nine RPE modified binders, with and without RET additives. When RPE alone was used for asphalt modification, the softening point difference between the top and bottom portions of each modified binder increased as the RPE dosage increased, indicating increased severity of phase separation. At 4% and 5% RPE dosages, the modified binders failed the GDOT requirement of a maximum allowable difference of 10°C. Figure 10 presents a fluorescent microscopy of the 5% RPE modified binder under a Zeiss Axiovert 200 Inverted Microscope, where the lighter color represents the RPE polymer-rich phase and the darker color represents the asphalt-rich phase. As can be seen, there were several isolated polymer coalescences caused by the physical separation and agglomeration of RPE particles from the binder. It was also observed that when this RPE modified binder cooled to room temperature, a film of RPE particles floated and agglomerated at the top of the binder sample. Both this observation and the fluorescence micrograph indicated the poor compatibility of the 5% RPE modified binder, which agreed with the storage stability result presented in Table 2.

At 3% RPE dosage, adding the two RET additives increased the softening point of both the top and bottom binder samples but did not significantly affect the final storage stability results. Both of the 3% RPE+RET modified binders passed the GDOT requirement. The 4% RPE modified binder showed a significant deterioration in storage stability when the RET1 additive was added; the resultant binder failed the GDOT requirement with a difference in the softening point of over 32°C. However, a different trend was observed for the RET2 additive, where the 4% RPE+RET2 modified binder marginally passed the test requirement. These results indicated that the RET2 additive was more effective in mitigating the phase separation of RPE modified binders than the RET1 additive. Nevertheless, the RET2 additive failed to accommodate the use of 5% RPE for asphalt modification; the final modified binder had a difference in the softening point of over 28°C, and thus, failed the GDOT requirement. The five modified binders passing the GDOT storage stability requirement were further evaluated in the study.

Table 2. Storage Stability Results

Binder ID	R&B Softening Point (°C)			Pass/Fail GDOT Requirement
	Top	Bottom	Difference	
2% RPE	46	43	3	Pass
3% RPE	47	44	3	Pass
4% RPE	60	45	15	Fail
5% RPE	80+ *	48	32+	Fail
3% RPE + RET1	54	52	2	Pass
4% RPE + RET1	80+ *	48	32+	Fail
3% RPE + RET2	54	52	2	Pass
4% RPE + RET2	57	48	9	Pass
5% RPE + RET2	80+ *	52	28+	Fail

*Note: * Exceeds the upper temperature range of the ASTM low softening point thermometer*

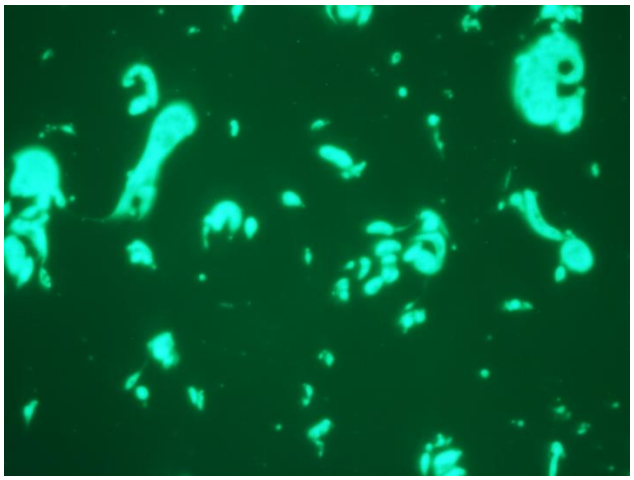

Figure 10. Fluorescence Micrograph of 5% RPE Modified Binder without RET Additives

However, during the later course of the project, the conventional storage stability procedure based on softening point test was found not sufficient to fully assess the phase separation tendency of PMA binders. Therefore, a modified test procedure based on MSCR testing of cigar tube portions was conducted on selected RPE and RPE+RET modified binders at WRI. Figure 11 presents the MSCR results at 58°C and 0.1 kPa stress level, for the top and bottom third-portions of the cigar tube samples after storage stability conditioning. As shown, both neat and RET modified binders had similar J_{nr} and %R values for the top and bottom samples. On the other hand, RPE and RPE+RET modified binders showed different MSCR results (i.e., lower J_{nr} and higher strain recovery values) between the top and bottom samples, indicating polymer separation. Figure 12 presents the MSCR results at 58°C and 3.2 kPa stress level, which confirms similar trends and findings in Figure 11. Adding RET to the RPE modified binder decreased the severity of phase separation but did not eliminate the problem at the tested dosage and conditions. Based on the storage stability results in Table 2, Figure 11, and Figure 12, MSCR testing of cigar tube portions seemed to provide better assessment of polymer separation of modified binders compared to the conventional test method using softening point test.

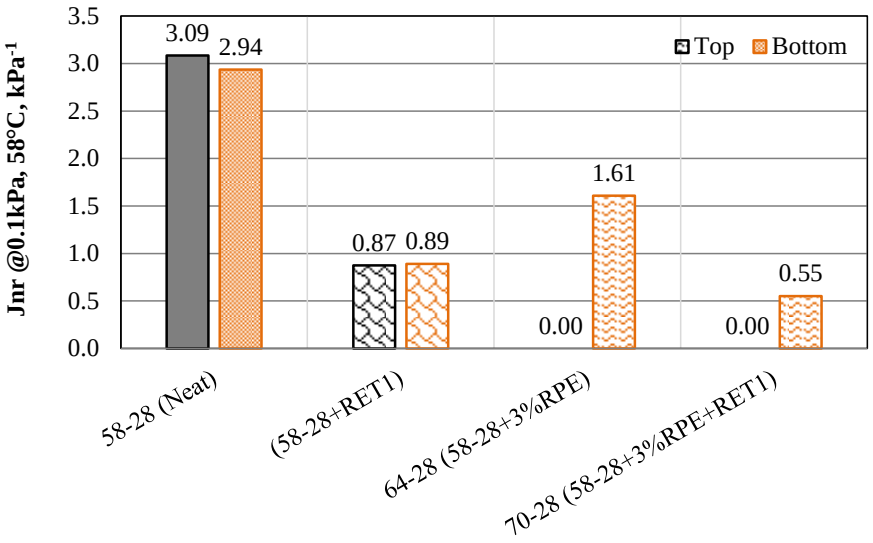

(a)

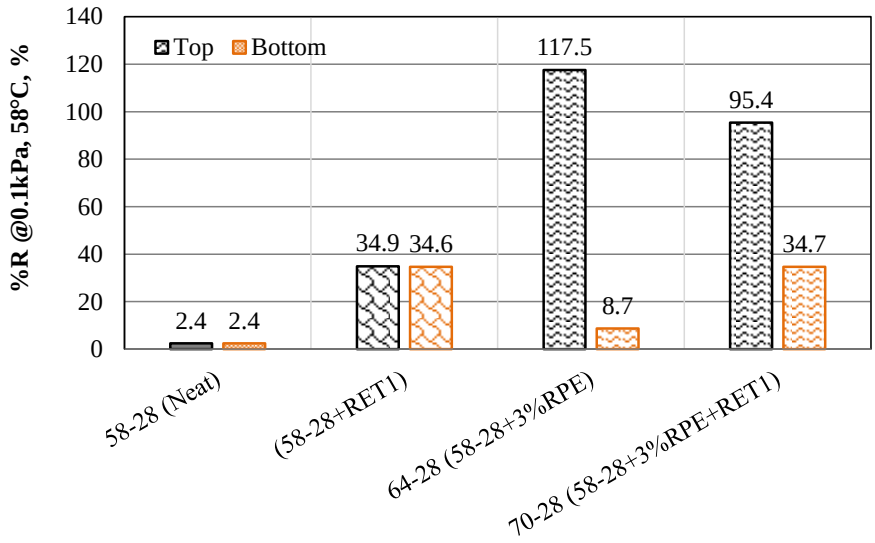

(b)

Figure 11. MSCR Results of Cigar Tube Portions at 58°C and 0.1 kPa; (a) $J_{nr,0.1}$, (b) $\%R_{0.1}$

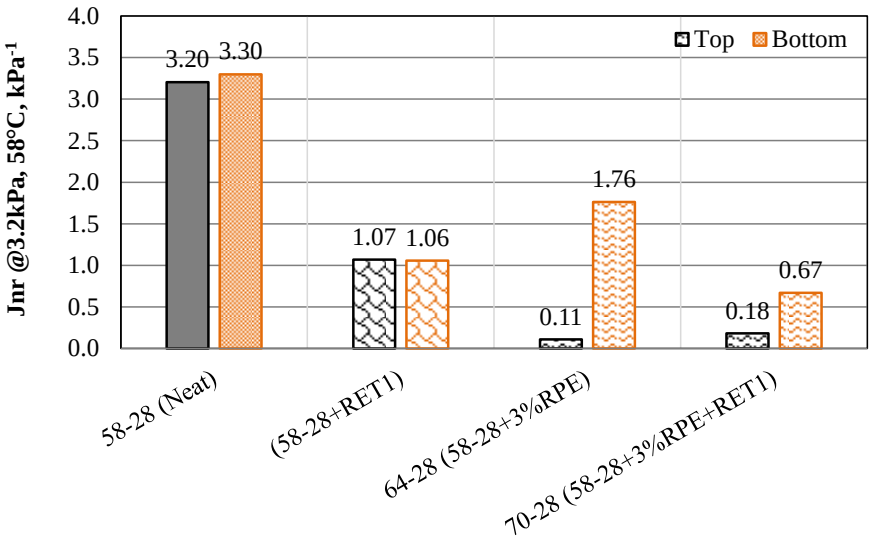

(a)

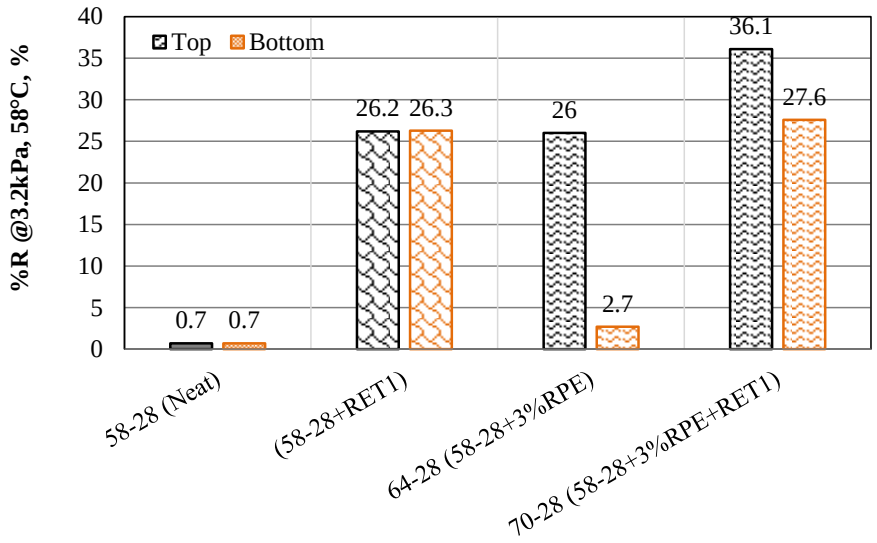

(b)

Figure 12. MSCR Results of Cigar Tube Portions at 58°C and 3.2 kPa; (a) $J_{nr,3.2}$, (b) $\%R_{3.2}$

4.2 Superpave PG and ΔT_c

Table 3 presents the Superpave PG results of the neat PG 58-28 binder and five RPE and RPE+RET modified binders that passed the storage stability test based on GDOT requirement. As shown, adding 2% and 3% RPE alone increased the continuous high-temperature grade of the binder, indicating potential improvement in binder rutting resistance. Both RPE modified binders had a high-temperature performance grade of 64°C, which was 6°C higher than that of the neat binder. Adding the two RET additives further enhanced the stiffness and rutting resistance of the RPE modified binder. The 3% RPE+RET1 modified binder had a high-temperature grade of 70°C, while the other two binders containing the RET2 additive passed the DSR $|G^*|/\sin(\delta)$ criteria at 76°C.

According to the BBR results, adding RPE alone or RPE plus RET additives did not have a significant effect on the binder low-temperature cracking resistance. All RPE modified binders with and without RET additives had the same low-temperature performance grade (i.e., -28°C) as the neat binder. No significant difference in the 20-hour PAV ΔT_c results was observed between the neat and RPE modified binders. However, BBR testing on selected 40-hour PAV aged samples indicated that the neat PG 58-28 binder had the highest (i.e., least negative) ΔT_c value of -1.4°C, followed by the 3% RPE modified binder (-2.4°C), and then the 3% RPE+RET1 modified binder (-4.9°C). In summary, the addition of RPE alone or RPE plus RET additives significantly improved the rutting resistance of asphalt binder but had no effect on its thermal cracking resistance and stress relaxation property after 20 hours of oxidative aging in PAV.

Table 3. Superpave PG and ΔT_c Results

Binder ID	Continuous Grade		20-hour PAV ΔT_c (°C)	Superpave PG
	High-Temp.	Low-Temp.		
Neat 58-28	61.2	-30.7	1.1	58-28
2% RPE	64.8	-29.7	1.3	64-28
3% RPE	67.2	-29.5	0.2	64-28
3% RPE + RET1	73.5	-30.6	0.3	70-28
3% RPE + RET2	76.8	-29.9	0.4	76-28
4% RPE + RET2	76.7	-29.3	0.1	76-28

4.3 MSCR

Figure 13 presents the MSCR results of the neat PG 58-28 binder and five RPE and RPE+RET modified binders at a test temperature of 64°C. For performance comparison, two SBS modified binders with similar PG and ΔT_c as the RPE and RPE+RET modified binders were tested; one binder contained 2.4% linear SBS polymer and had a PG of 64-28 and ΔT_c of 1.0°C and the other binder contained 4.2% linear SBS polymer and had a PG of 70-28 and ΔT_c of -0.2°C. As shown in Figure 13(a), the 2% and 3% RPE modified binders had negligible $\%R_{3.2}$ values (less than 3.0%) at 64°C, indicating that virtually all the shear strain accumulated in the MSCR test was non-recoverable. On the other hand, the three RPE modified binders containing the RET additives had significantly higher $\%R_{3.2}$ values, indicating enhanced binder elasticity due to the additives. Nevertheless, when comparing the two PG 70-28 binders, the 3% RPE+RET1 modified binder performed similarly to the SBS binder. In Figure 13(b), both the 2% and 3% RPE modified binders had significantly lower $J_{nr,3.2}$ values than the neat PG 58-28 binder, indicating the effect of RPE modification on improving the rutting resistance of asphalt binder. Adding RPE and RET in combination offered further improvement; the RPE+RET modified binders had similar $J_{nr,3.2}$ values to the SBS modified binders, which were significantly lower than those of the RPE modified binders.

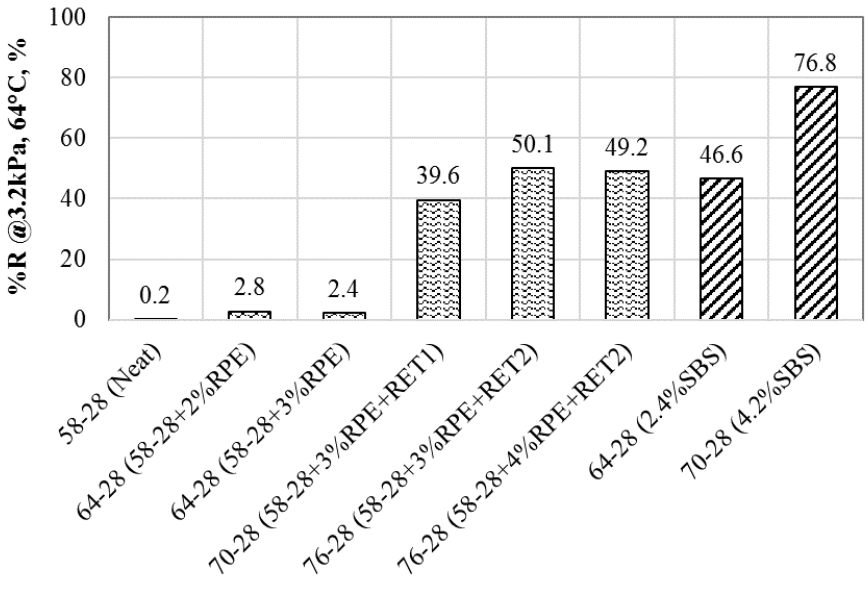

(a)

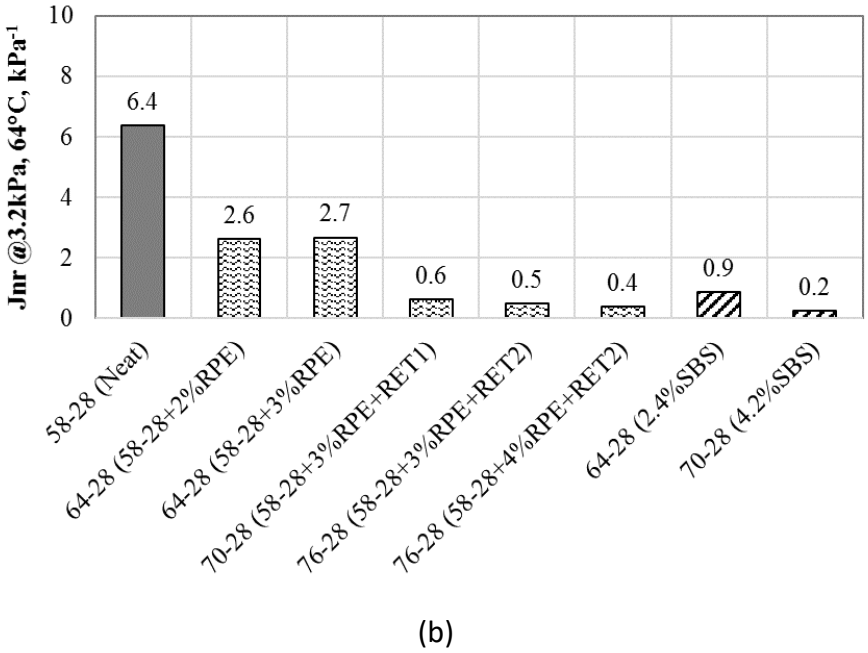

(b)

Figure 13. MSCR Results of RPE and RPE+RET Modified Binders versus Neat and SBS Modified Binders; (a) $\%R_{3.2}$, (b) $J_{nr,3.2}$

4.4 LAS

Figure 14 presents the comparison in LAS results of RPE and RPE+RET modified binders versus the neat PG 58-28 binder and two SBS modified binders. At both 2.5% and 5.0% strain levels, the 2% and 3% RPE modified binders had similar N_f values as the neat binder, which were lower than that of the SBS modified PG 64-28 binder. These results indicated that the use of RPE alone for asphalt modification had no improvement on the fatigue resistance of asphalt binder. However,

when RPE and RET were used in combination, the modified binders showed substantially higher N_f values and thus, potential longer fatigue lives than the neat binder. Such improvement in fatigue resistance was mainly due to the enhanced fatigue tolerance and overall flexibility provided by the elastomeric RET additives. When comparing the two PG 70-28 modified binders, the one containing 3% RPE plus the RET1 additive outperformed the SBS modified binder.

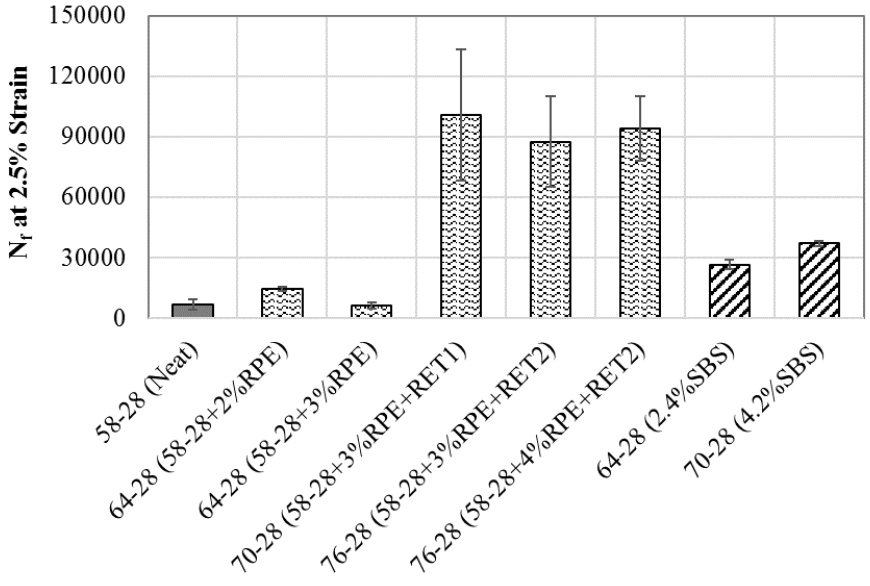

(a)

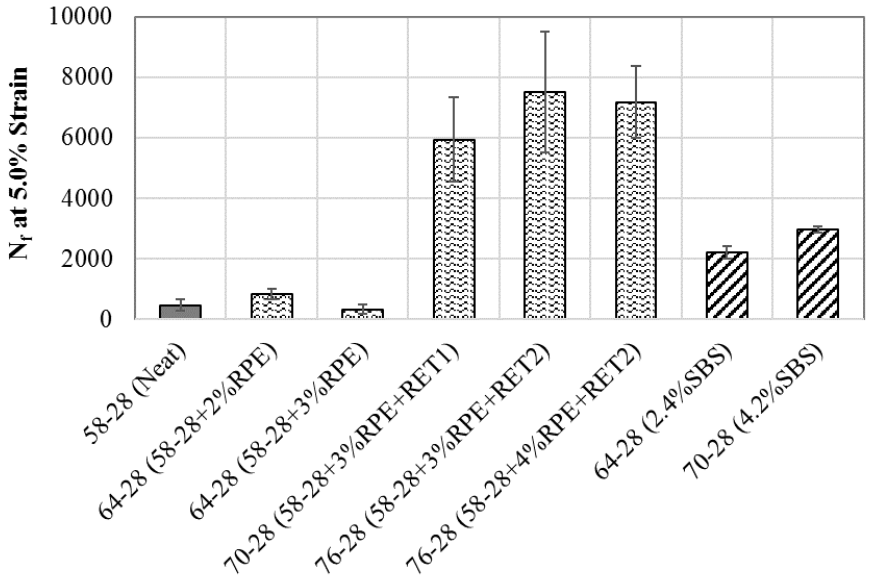

(b)

Figure 14. LAS Results of RPE and RPE+RET Modified Binders versus Neat and SBS Modified Binders; (a) N_f at 2.5% Strain, (b) N_f at 5.0% Strain

4.5 G-R Parameter

Table 4 summarizes the G-R parameter results of the neat and RPE and RPE+RET modified binders at three aging conditions: unaged, after RTFO aging, and after PAV aging. As shown, the RPE+RET modified binders consistently showed the highest G-R parameters, followed by the RPE modified binders and then the neat binder. These results highlighted the binder stiffening effect due to the use of RPE and RET for asphalt modification. Nevertheless, none of the RPE and RPE+RET modified binders exceeded the preliminary G-R parameter criterion of 180 kPa for the onset of block cracking after 20 hours of PAV aging; and thus, the possibility of these modified binders having premature block cracking in the field is low. However, debate exist in the validity of using the G-R threshold for evaluating PMA binders.

Table 4. G-R Parameter Results of Neat, RPE Modified, and RPE+RET Modified Binders

Binder ID	G-R Parameter (kPa)		
	Unaged	RTFO-aged	PAV-aged
Neat 58-28	0.2	0.7	20.9
2% RPE	0.2	2.3	39.4
3% RPE	0.8	4.1	49.3
3% RPE + RET1	1.8	12.2	111.6
3% RPE + RET2	1.8	6.3	63.6
4% RPE + RET2	2.6	10.4	136.1

Figure 15 presents the G-R parameter results on a Black Space diagram, where the binder $|G^*|$ at 15°C and 0.005 rad/s is plotted on the y-axis versus δ at the same condition on the x-axis. The two dashed curves in the figure represent the two preliminary G-R parameter criteria of 180 kPa and 600 kPa for the onset of block cracking and significant cracking, respectively. As shown, adding 2% and 3% RPE alone increased binder $|G^*|$ but decreased δ. As a result, the RPE modified binders had higher G-R parameters than the neat binder and were located closer to the "cracking damage zones" on the Black Space diagram. Compared to the RPE modified binders, RPE+RET modified binders had similar $|G^*|$ but lower δ, which resulted in higher G-R parameters and a horizontal shift of the data points to the left of the diagram. Again, none of the RPE or RPE+RET modified binders reached the preliminary G-R parameter criterion of 180 kPa after 20 hours of PAV aging.

Finally, the G-R ratio results were determined to evaluate the effect of RPE modification on the aging resistance of asphalt binder. For each binder, the G-R ratio was calculated as the fraction of the G-R parameter of the PAV-aged sample over that of the RTFO-aged sample. As shown in Figure 16, both RPE and RPE+RET modified binders had lower G-R ratios than the neat PG 58-28 binder, indicating reduced susceptibility to oxidative aging. Among the three PG 64-28 binders, the SBS modified binder exhibited the lowest G-R ratio than the two binders modified with 2% and 3% RPE. A similar trend was also observed for the two PG 70-28 binders, where the SBS modified binder outperformed the 3% RPE+RET modified binder in terms of aging resistance.

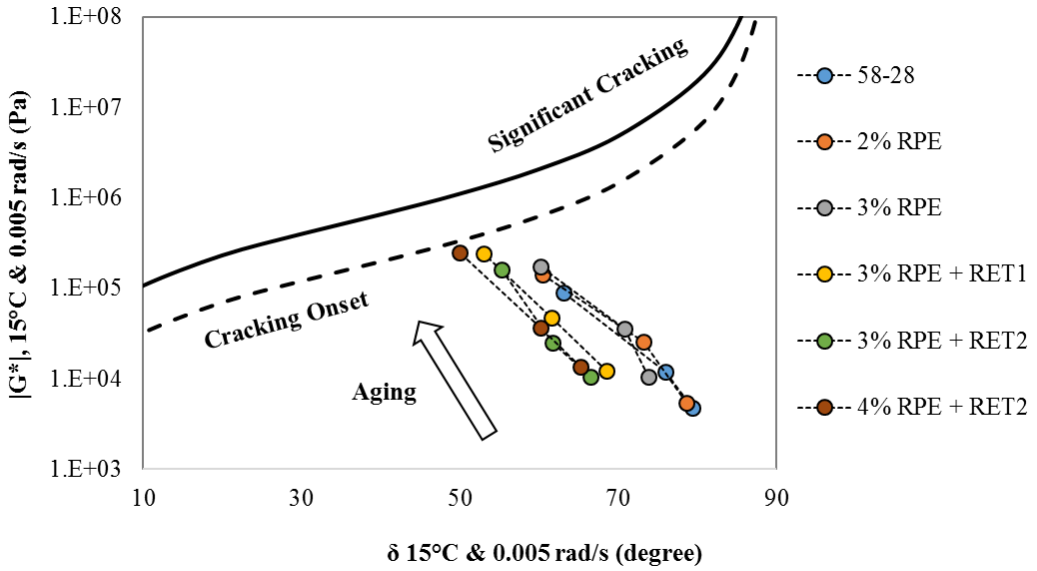

Figure 15. G-R Parameter Results of Neat, RPE Modified, and RPE+RET Modified Binders on a Black Space Diagram

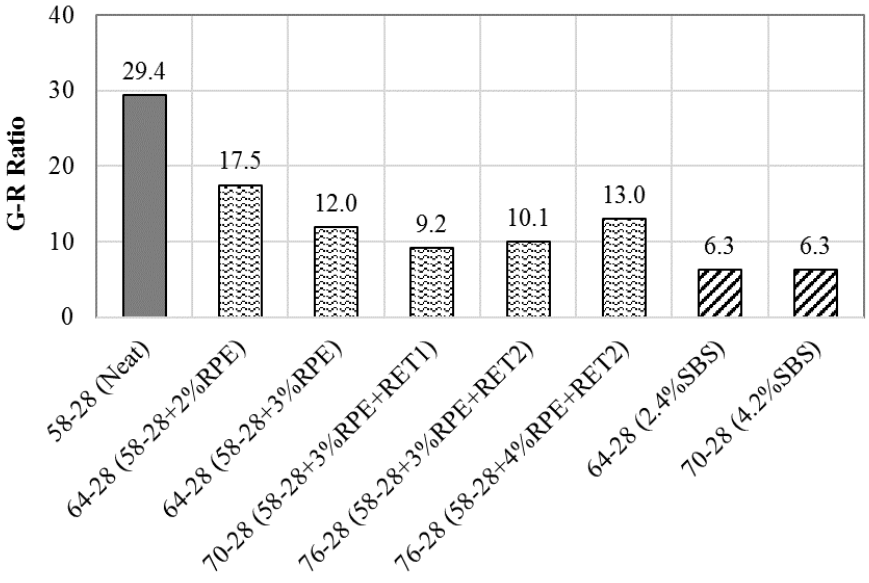

Figure 16. G-R Ratio Results of RPE and RPE+RET Modified Binders versus Neat and SBS Modified Binders

5. BINDER CEHMICAL ANALYSIS RESULTS

5.1 RPE Solubility

As shown in Figure 17, the RPE sample tested in the study was insoluble in Tetrahydrofuran (THF), Dichloromethane (DCM), and Chlorobenzene (CB), which are solvents commonly used in chromatography and spectroscopy characterization techniques. This observation complicated the chemical characterization of RPE modified asphalts and raised concerns about the chemical

compatibility of RPE in the asphalt colloidal system. Therefore, further research efforts are needed to investigate the compatibility between RPE and asphalt binders.

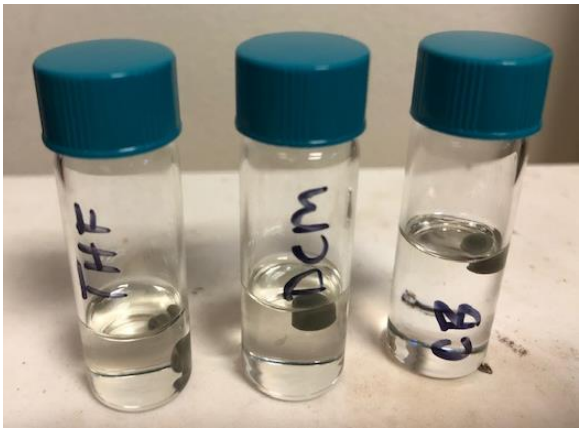

Figure 17. Insolubility of RPE in Various Solvents [From left to right: Tetrahydrofuran (THF), Dichloromethane (DCM), and Chlorobenzene (CB)]

5.2 FT-IR ATR

Figure 18 presents the FTIT-ATR spectra of the RPE additive, neat PG 58-28 binder, and an RPE modified binder. As can be seen, the RPE polymer showed CH_2 bend peaks at 1472 and 1462 cm^{-1}. However, these peaks cannot be easily used to diagnose the RPE modified binder because the neat binder contained functional groups that overlapped with these two peaks. No significant differences were observed between the FTIR spectra of the neat and RPE modified binders. Figure 19 shows the peak characteristic of carbonyl stretching, which can be associated with the RET additive when comparing the RET modified binder versus the neat binder.

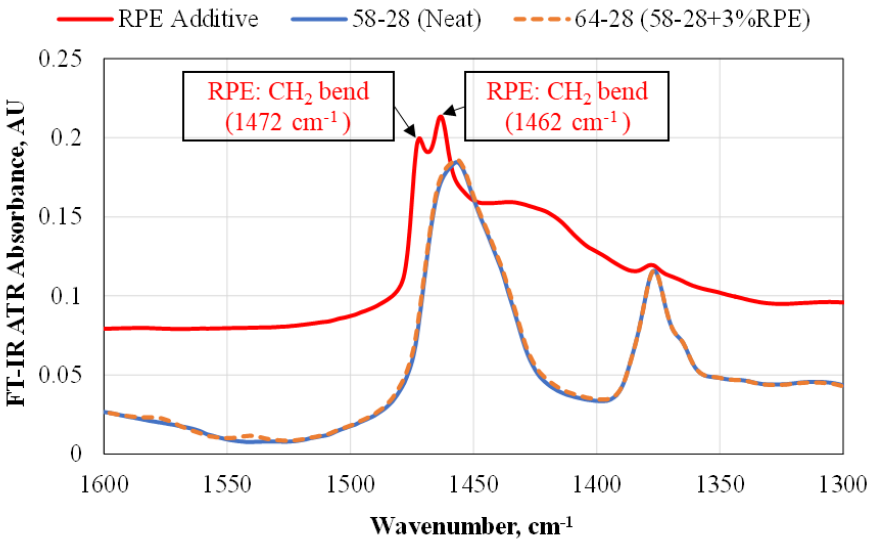

Figure 18. FT-IR ATR Absorbance of RPE Additive and Neat versus RPE Modified Binders

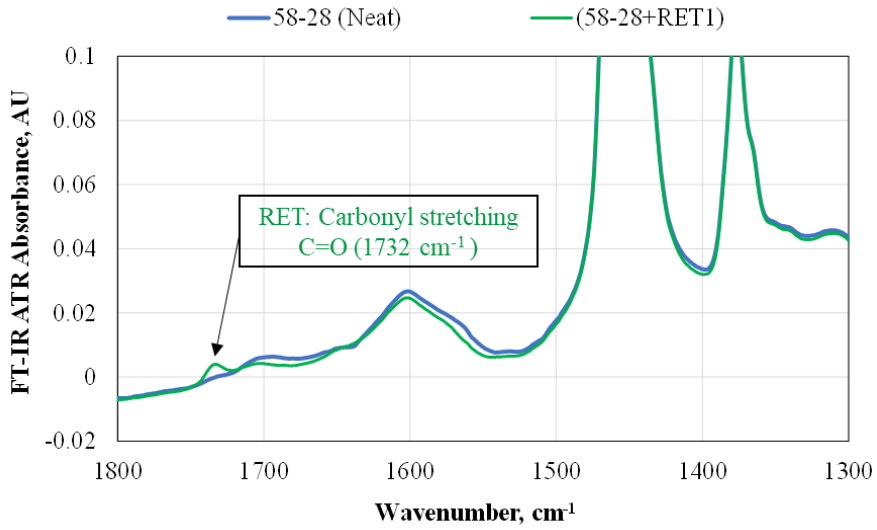

Figure 19. FT-IR ATR Absorbance of Neat versus RET Modified Binders

5.3 DSC

Figure 20 presents the reversed capacity curves of the RET, RPE, RPE+RET modified binders compared to the neat binder. As can be seen, the melting onset temperature of RPE was found at 114.7°C.

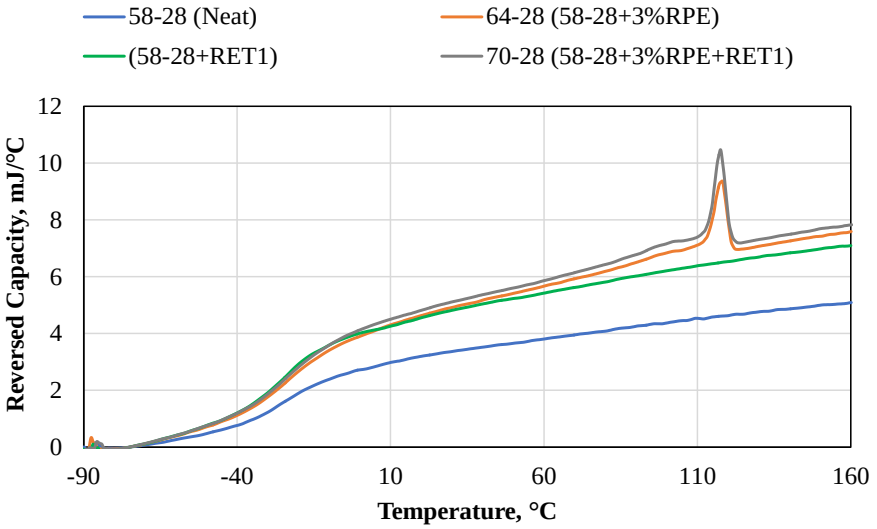

Figure 20. Unmodulated DSC Reversing Capacity Curves

Table 5 shows the melting temperature observed during the heating cycle at 10°C/min and the crystallization onset temperature, when cooling at 5°C/min from the total heat flow curves. The amount of crystallizable fractions was determined assuming that pure wax has a crystallization energy of 180 J/g. As indicated in Table 5, the neat binder showed no crystallizable fractions or waxes; therefore, the crystallizable fraction reported for the RPE and RPE+RET modified binders corresponded to the RPE crystallization.

Table 5. Crystallization/Melting Parameters from Unmodulated DSC

Binder ID	Unmodulated DSC – Cooling Ramp			Heating Ramp	
	Cryst. Onset	Exo. Area	% Crystallizable Fraction	Melting Onset	Endo. Area
	°C	J/g	%	°C	J/g
58-28 (Neat)	-	-	-	-	-
(58-28+RET1)	-	-	-	-	-
64-28 (58-28+3%RPE)	106.1	3.72	2.07	114.7	1.91
70-28 (58-28+3%RPE+RET1)	106.4	3.74	2.08	114.6	1.73

Table 6 summarizes the glass transition temperatures of the neat, RET modified, RPE modified, and RPE+RET modified binders. $T_{g,}$ onset is the temperature at which the material is a complete elastic solid and begins to undergo molecular motions. $T_{g,}$ endpoint is the temperature at which all molecules have complete vibrational and rotational motion. $T_{g,}$ width is the difference between the $T_{g,}$ onset and $T_{g,}$ endpoint. The center of the glass transition region is determined by two parameters; $T_{g,}$ (I) at the inflection point between the T_g, onset and T_g, endpoint, and T_g, (H) at the half-height between the heat flow of T_g, onset and T_g, endpoint. As can be seen, the RPE modified binders showed warmer (i.e., less negative) T_g, (I) and T_g, (H). Furthermore, a relatively larger T_g width was observed for the RPE modified binders, which could be an indication of a more complex system in comparison to the neat binder.

Table 6. Glass Transition Parameters from Modulated DSC

Binder ID	Modulated DSC				
	Tg, (Half- Height)	Tg, (Inflection point)	Tg, Onset	Tg, end point	Tg, Width
	°C	°C	°C	°C	°C
58-28 (Neat)	-21.7	-24.4	-38.9	-4.4	34.5
(58-28+RET1)	-23.1	-25.1	-38.4	-7.9	30.4
64-28 (58-28+3%RPE)	-19.8	-23.8	-38.0	-1.5	36.6
70-28 (58-28+3%RPE+RET1)	-20.0	-22.7	-39.1	-1.1	38.1

5.4 SAR-AD™ Fractions

As previously discussed in Section 5.1, the RPE sample was found insoluble in chlorobenzene (CB), which is the injecting solvent used in SAR-AD procedure. Thus, RPE was considered as part of a 9th fraction of toluene-insoluble materials that would be filtered before the sample being injected into the SAR-AD columns. Figure 21 shows the filters used to separate toluene-insoluble materials for (A) neat, (B) RET modified, (C) RPE modified, and (D) RET+RPE modified binders. The weight percentage of the toluene-insoluble materials where 0.2% for neat binder, 0.5% for RET modified binder, 14.2% for RPE modified binder, and 26.3% for RET+RPE modified binder.

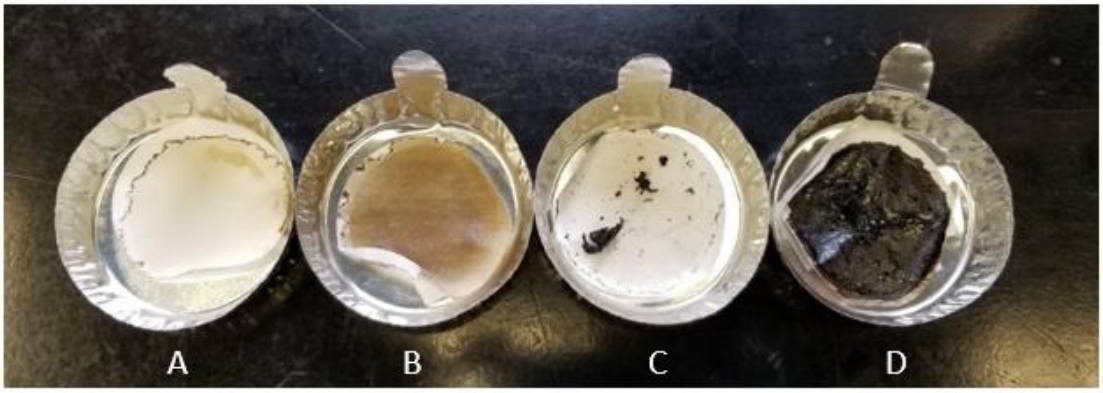

Figure 21. Filtered Materials for (A) Neat, (B) RET Modified, (C) RPE Modified, and (D) RET+RPE Modified Binders

Table 8 presents the contents of the eight asphalt fractions determined using the SAR-AD procedure. In addition, Table 8 shows two parameters: (1) Coking Index (C6/CCl), which represents the ratio of the least polar cyclohexane-soluble asphaltenes to the most polar methylene chloride-soluble asphaltenes, and (2) Colloidal Instability Index (CII), which is the ratio of the incompatible materials (saturates + asphaltenes) to the solubilizing materials (aromatics + resins). Since RPE was found insoluble in chlorobenzene, the eight ELSD fractions for the RPE modified binders were adjusted to account for the weight percentage of the 9^{th} fraction that would be filtered before the sample was injected into the SAR-AD columns. Table 8 summarizes the nine fractions from SAR-AD and filtration.

Table 7. SAR-AD Fractions (ELS and 500 nm Detectors)

Sample ID	Det	Maltenes						Asphaltenes				Coking Index	CII
		Sat	Aro 1	Aro 2	Aro 3	Total Aro	Resins	CyC_6	Toluene	CH_2Cl_2: MeOH	Total ELSD Asphaltenes	C_6/CCl	
58-28 (Neat)	ELS	12.2	5.9	25.0	32.6	63.5	11.5	4.3	8.4	0.1	12.8		0.3
	500 nm			0.2	16.4		21.7	19.7	40.2	1.7		11.5	
(58-28+RET1)	ELS	12.3	6.0	25.6	32.4	64.0	11.3	3.2	8.6	0.6	12.4		0.3
	500 nm			0.2	17.2		19.8	15.0	41.9	5.8		2.6	
64-28 (58-28+3%RPE)	ELS	13.2	5.4	27.7	30.7	63.8	11.7	4.0	7.2	0.1	11.3		0.3
	500 nm			0.2	17.2		22.0	20.3	38.7	1.5		13.2	
70-28	ELS	14.3	5.6	27.9	32.2	65.7	11.0	2.7	6.0	0.2	9.0		0.3
(58-28+3%RPE+RET1)	500 nm			0.2	18.8		23.0	16.9	37.9	3.2		5.3	

Table 8. SAR-AD ELSD Adjusted Eight Fractions and the Ninth Fraction of Toluene-Insoluble Filtered Materials

Sample ID	Adjusted Maltenes						Adjusted Asphaltenes				Insolubles (9^{th} Fraction)
	Sat	Aro 1	Aro 2	Aro 3	Total Aro	Resins	CyC_6	Toluene	CH_2Cl_2: MeOH	Total ELSD Asphaltenes	
58-28 (Neat)	12.2	5.8	25.0	32.6	63.4	11.5	4.3	8.4	0.1	12.8	0.2
(58-28+RET1)	12.3	6.0	25.5	32.2	63.7	11.3	3.2	8.5	0.6	12.3	0.5
64-28 (58-28+3%RPE)	11.3	4.7	23.8	26.3	54.8	10.1	3.4	6.2	0.1	9.7	14.2
70-28 (58-28+3%RPE+RET1)	10.5	4.1	20.6	23.7	48.4	8.1	2.0	4.4	0.2	6.6	26.3

Figure 22 presents a graphical representation of the nine fractions, shown in Table 8, for the neat, RET modified, RPE modified, and RPE+RET modified binders. As can be seen, a larger amount of toluene-insoluble material was found for the RPE+RET modified binder (26.3% by weight) in comparison to the RPE modified binder (14.2% by weight). These results could be an indication that the storage stability test does not directly represents the evaluation of chemical compatibility of polymer modified binders.

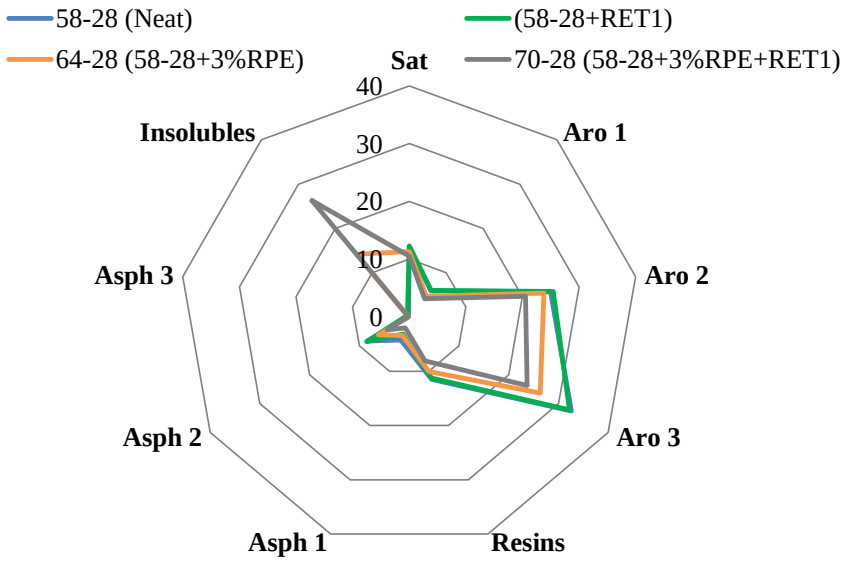

Figure 22. SAR-AD ELSD Adjusted Eight Fractions and the Ninth Fraction of Toluene-Insoluble Filtered Materials

5.5 GPC Chromatograms

Figure 23 presents the RI chromatograms for RET, RPE, and RPE+RET modified binders versus the neat binder. As previously discussed, lower retention times are equivalent to higher apparent molecular weight. Recalling that a significant portion of the RPE and RPE+RET modified binders was insoluble in the selected injecting solvent, the collected total response (i.e., area under the curve) of the RPE and RPE+RET modified binders was lower than the total response obtained for the binders without RPE. Furthermore, the combination of RET and PPA seemed to affect the molecular association of the asphaltenes as well as their apparent molecular weight, leading to a less prominent shoulder compared to that of the neat binder at low retention time (i.e., 16.5 minutes).

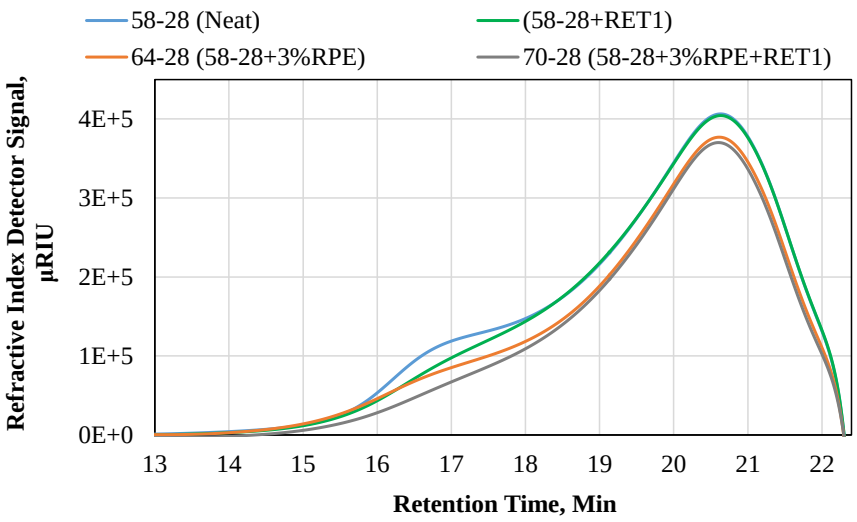

Figure 23. GPC/SEC Refractive Index Detector Chromatograms for Neat, RET Modified, RPE Modified, and RPE+RET Modified Binders

6. MIXTURE PERFORMANCE TEST RESULTS

6.1 BBS Test

Figure 24 presents the dry bond strength results before and after oxidative aging in PAV. As can be seen for all binders tested, a higher bond strength was observed after oxidative aging. This phenomenon can be explained by the fact that the presence of carboxylic acids, which are products of asphalt oxidation, being quite polar and therefore adhering strongly to dry aggregate, resulted in higher POTS values in the BBS test. With exception of the unaged 3% RPE3+RET2 modified binder, the RPE and REP+RET modified binders showed lower dry bond strength values in comparison to the neat and SBS modified binders.

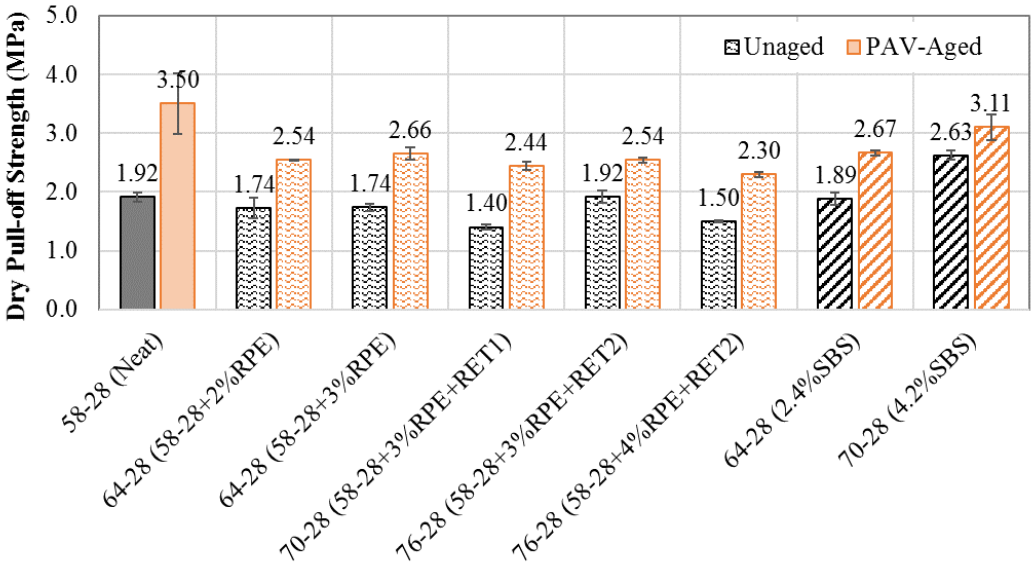

Figure 24. Dry Bond Strength of Unaged and PAV-Aged Asphalt Binders

Figure 25 presents the wet bond strength results before and after oxidative aging in PAV. Note that moisture damage is a time-dependent phenomenon, and thus, an indirect way to investigate this time-dependency behavior is to measure the variation in the bond strength with time in the presence of water. As can be seen for all binders tested, a decrease in the bond strength was observed after 48 hours of moisture conditioning before and after oxidative aging in the PAV. However, the reduction in POTS after moisture conditioning was more significant for the PAV aged samples, which was likely due to the fact that the carboxylic groups produced during oxidation (i.e., sodium and potassium salts of carboxylic acids in asphalt) tended to be easily removed from the aggregate in the presence of water (*Robertson, 2000*). This effect was more accentuated for binders modified with RPE alone.

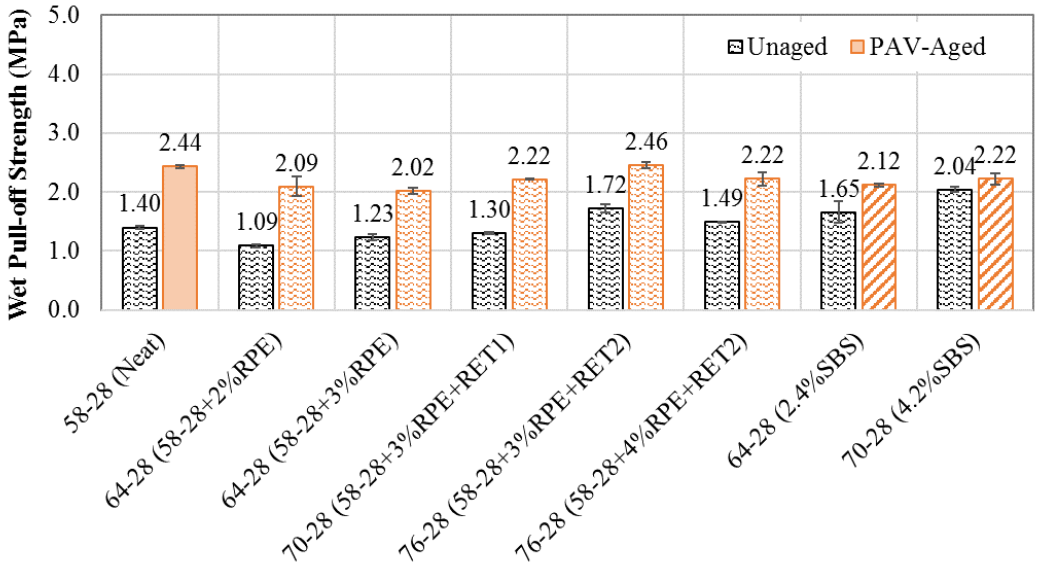

Figure 25. Wet Bond Strength of Unaged and PAV-Aged Asphalt Samples After 48 Hours of Moisture Conditioning

Figure 26 shows the loss of bond strength of the unaged and PAV-aged asphalt binders, which is indicative of the moisture sensibility of the asphalt-aggregate system. The loss of bond strength was calculated in accordance to Equation 9. As can be seen, before oxidative aging in PAV, the binders modified with RPE-only showed the highest loss of bond strength in comparison to the neat, SBS modified, and RPE+RET modified binders. On the other hand, the RPE+RET modified binders showed the highest resistance to moisture damage in comparison with all other binders before and after aging. Note, however, that this behavior did not only refer to the use of RPE and RET for asphalt modification, but it was also guided by the incorporation of PPA additive because PPA action is known to reduce the moisture susceptibility of granite aggregates, which are acidic in nature.

$$Loss\ of\ Bond\ Strength = \frac{POTS_{dry} - POTS_{48hrs,wet}}{POTS_{dry}} * 100\% \qquad \text{Equation 9}$$

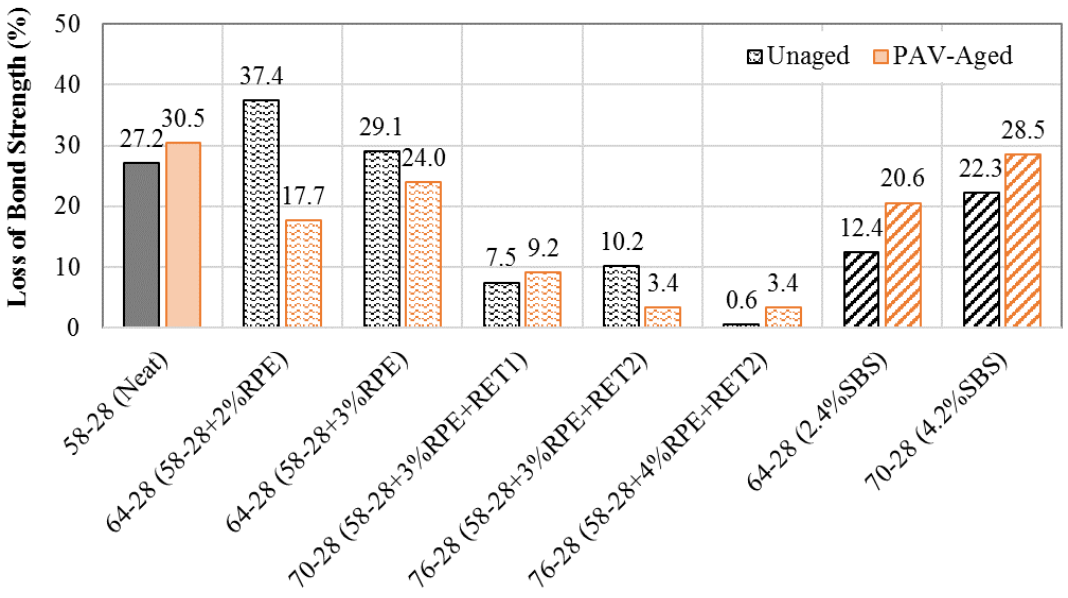

Figure 26. Loss of Bond Strength After 48 Hours of Moisture Conditioning

6.2 HWTT

Figure 27 presents the HWTT rut depth curves of the four mixtures tested in the study. Note that these mixtures were tested after short-term aging for four hours at 135°C. In general, the mixtures containing RPE, RPE+RET, and SBS modified binders significantly outperformed the control mixture with a neat PG 58-28 binder. The unmodified control mixture exhibited a stripping phase on the HWTT curve, which indicated that stripping of asphalt binders from aggregates occurred during the test.

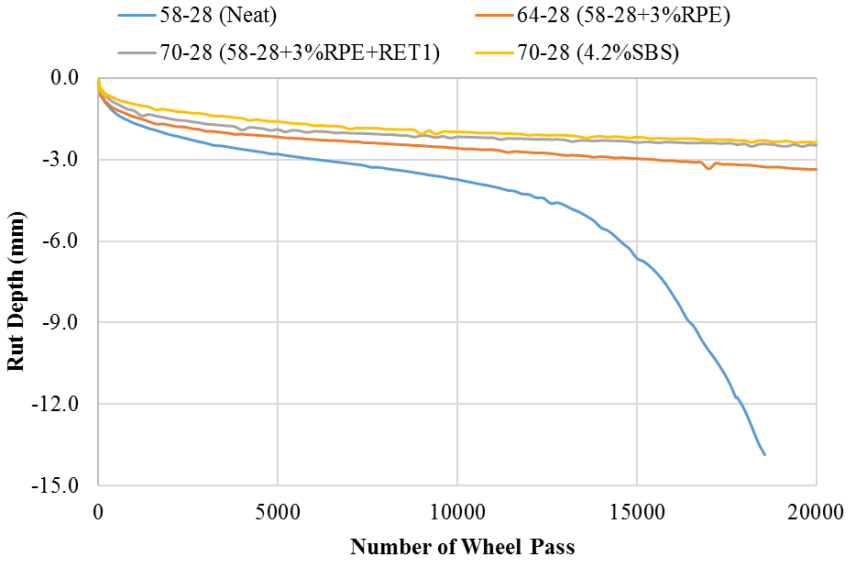

Figure 27. HWTT Rut Depth Curves

Figure 28 presents the calculated average HWTT CRD_{20k} and *RRI* results. As can be seen in Figure 28(a), the CRD_{20k} results decreased as the binder's high-temperature PG increased.

Specifically, the two mixtures containing RPE+RET and SBS modified binders had the lowest CRD_{20k} values, and thus, best rutting resistance, followed by the RPE modified mixture and then the unmodified control mixture. A similar trend was also observed in Figure 28(b), where the three modified mixtures had significantly higher *RRI* values than the unmodified control mixture. These results indicated that using RPE and RPE+RET for asphalt modification improved the rutting resistance of asphalt mixtures and that the improvement due to adding RPE and RET in combination was comparable to SBS modified binder.

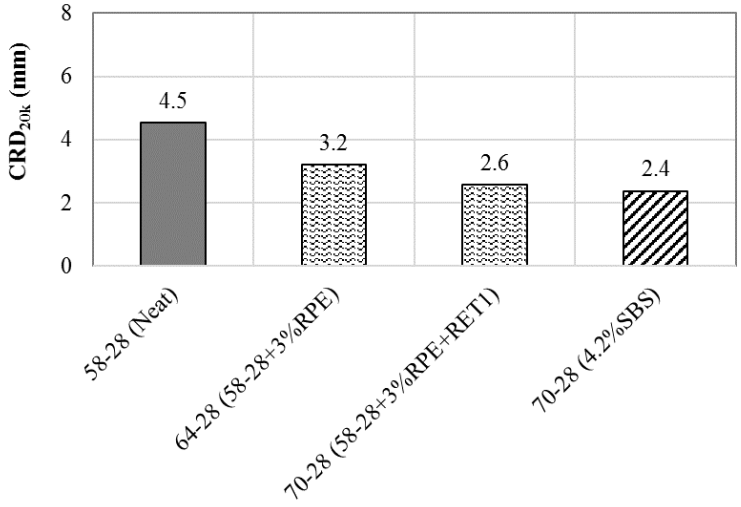

(a)

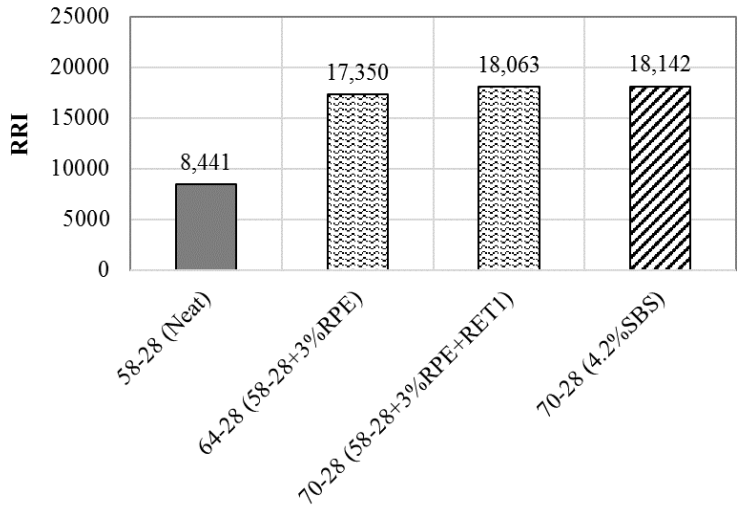

(b)

Figure 28. HWTT Results; (a) CRD_{20k}, (b) *RRI*

6.3 IDEAL-CT

Figure 29 presents the IDEAL-CT load versus displacement curves for four mixtures containing different types of asphalt binders in the study. Note that these mixtures were tested after loose mix long-term aging for eight hours at 135°C. In general, the RPE+RET modified mixture exhibited

a more brittle behavior than the other three mixtures, as indicated by a higher peak load and a steeper post-peak slope. Additionally, the PG 58-28 control mixture had a slightly lower peak load than the RPE and SBS modified mixtures, but their post-peak slopes were similar.

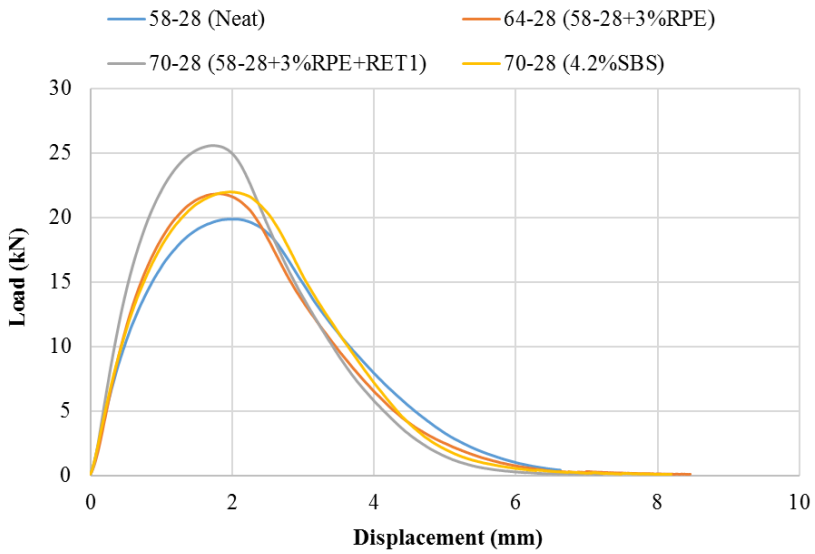

Figure 29. IDEAL-CT Load versus Displacement Curves

Figure 30 summarizes the calculated CT_{index} results, where the bars represent the average values and the whiskers denote the average plus and minus one standard deviation out of six replicates. The unmodified control mixture exhibited a higher average CT_{index} value than the three mixtures containing RPE, RPE+RET, and SBS modified binders, which indicates greater flexibility and better intermediate-temperature cracking resistance. Note that these results contradicted the binder LAS results in Figure 30, which was likely due to the fact that the LAS test was conducted at the binder's intermediate-temperature PG while the IDEAL-CT was tested at 25°C regardless of binder PG; as a result, the LAS test took into consideration equal binder stiffness while assessing the intermediate-temperature fatigue characteristics of different asphalt binders while the IDEAL-CT did not. The statistical analyses [i.e., analysis of variance (ANOVA) and Tukey's honest significance difference test (HSD)] identified a significant difference in the CT_{index} results between the unmodified control mixture and RPE+RET modified mixture, while the differences among other mixtures were not statistically significant. In summary, the IDEAL-CT results indicated that the use of RPE alone for asphalt modification had no effect on the intermediate-temperature cracking resistance of asphalt mixtures, while adding RPE and RET in combination showed a negative impact.

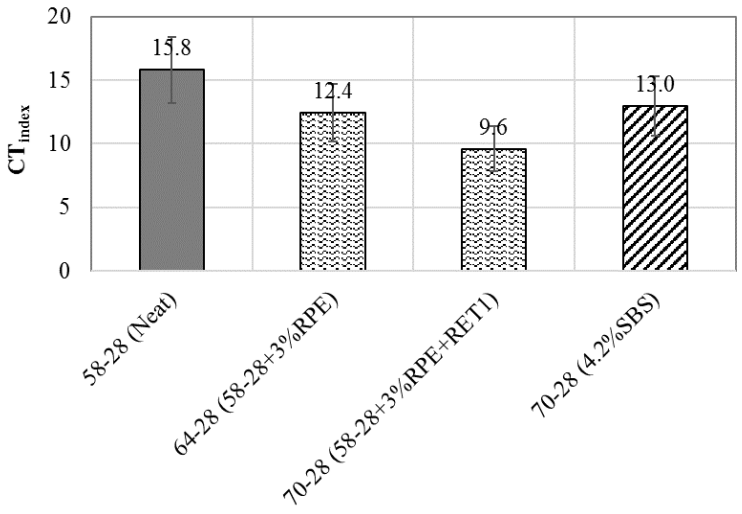

Figure 30. IDEAL *CT$_{index}$* Results

6.4 DCT Test

Figure 31 presents the DCT G_f results of the four mixtures tested in the study. Note that these mixtures were tested after loose mix long-term aging for six hours at 135°C. For the DCT G_f parameter, a higher value is indicative of better resistance to thermal cracking. As can be seen, the SBS modified mixture exhibited the highest average G_f value, followed by the unmodified control mixture, and then the two RPE and RPE+RET modified mixtures. However, the ANOVA test indicated that the difference among these four mixtures was not significant if considering the variability of the DCT G_f results. Therefore, the RPE and RPE+RET modified mixtures were expected to have equivalent thermal cracking resistance as those containing a PG 58-28 neat binder and an SBS modified binder. This finding is consistent with the binder's low-temperature PG results in Table 3.

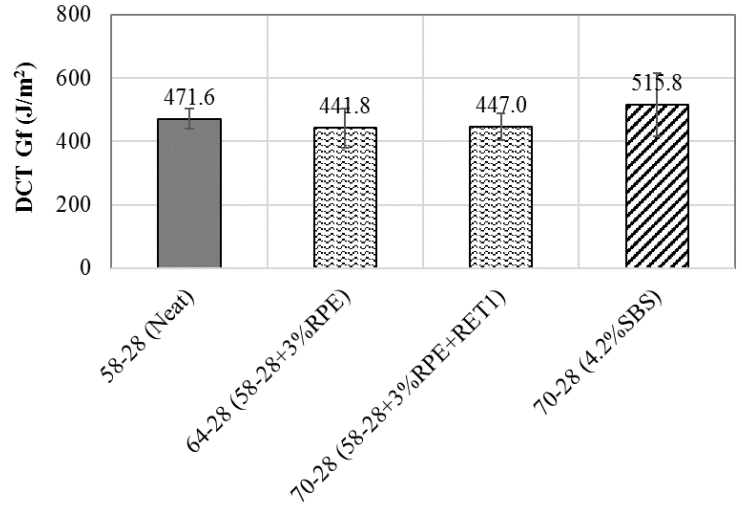

Figure 31. DCT G_f Results

6.5 OT

Figure 32 presents the OT results of the four mixtures containing different types of asphalt binders. Note that these mixtures were tested after loose mix long-term aging for eight hours at 135°C. For the OT β parameter, a lower value is indicative of better resistance to reflective cracking. As shown in Figure32, the unmodified control mixture had a lower average β value than the mixtures containing RPE, RPE+RET, and SBS modified binders. However, the differences were statistically insignificant, which indicated that using RPE and RPE+RET for asphalt modification had no significant impact on the reflective cracking resistance of asphalt mixtures.

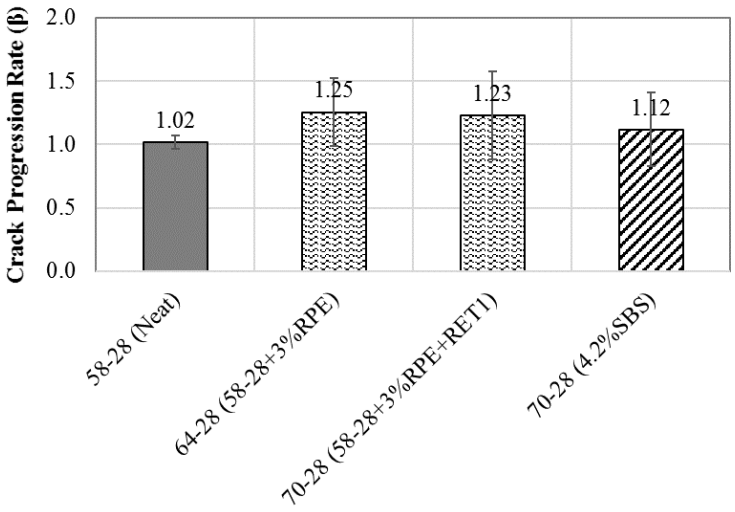

Figure 32. OT β Parameter Results

7. CONCLUSIONS AND FUTURE RESEARCH

This study sought to determine the feasibility of using RPE alone and RPE plus RET for asphalt modification and evaluate their impacts on the performance properties of asphalt binders and mixtures. To accomplish the research objectives, three laboratory experiments were conducted; the first experiment focused on storage stability, florescent microscopy, and rheology testing of RPE and RPE+RET modified binders. In the second experiment, analytical chemical analyses were conducted to determine the infrared spectroscopy, thermal properties, component fractions, and molecular weight distribution of selected RET and RET+RET modified binders in comparison to the neat and SBS modified binders. Finally, the last experiment focused on mixture performance testing to assess the impact of using RPE and RPE+RET for asphalt modification on the rutting, cracking, and moisture resistance of asphalt mixtures. Based on the results of the study, the following conclusions were made:

- Asphalt binders containing 2% and 3% RPE passed the GDOT storage stability requirement, while the modified binders containing higher RPE dosages (i.e., 4% and 5%) failed. Fluorescent microscopy of a 5% RPE modified binder confirmed the physical separation and chemical incompatibility between the RPE polymer and base binder used.

- Adding an ethylene-based RET additive improved the storage stability of RPE modified binders. The modified binder containing 4% RPE and the RET2 additive also passed the GDOT storage stability requirement.
- Some of the RPE and RPE+RET modified binders that passed the GDOT requirement showed phase separation issue when cooled to ambient temperature without shear agitation. This observation was confirmed in a modified storage stability test based on the MSCR testing of top versus bottom cigar tube portions.
- As compared to the conventional storage stability test method based on softening point test, MSCR testing on cigar tube portions seemed to provide better assessment of polymer separation of modified binders.
- Using 2% and 3% RPE for asphalt modification increased the stiffness and rutting resistance of asphalt binder but had no effect on its low-temperature cracking, fatigue cracking, and block cracking resistance.
- Using RPE plus RET for asphalt modification significantly increased binder elasticity, rutting resistance, and fatigue resistance, but had no impact on low-temperature cracking resistance.
- Both RPE and RPE+RET modified binders showed improved aging resistance over the neat binder. The improvement, however, was not as pronounced as SBS modified binders.
- RPE modified binders showed warmer (i.e., less negative) glass transition temperatures and relatively larger glass transition width, which could be an indication of a more complex system in comparison to the neat binder.
- DSC was found to be a useful tool for evaluating RPE modified binders. This technique was capable of determining the melting onset temperature of RPE.
- The RPE sample evaluated in the study was insoluble in solvents commonly used in chromatography and spectroscopy characterization techniques for polymers and asphalt binders. This observation complicated the chemical characterization of RPE modified binders and raised concerns about the chemical compatibility of RPE in the asphalt colloidal system.
- The RPE+RET modified binder had a higher amount of toluene-insoluble material than the RPE modified binder, which could potentially indicate that the storage stability test does not directly represents the evaluation of chemical compatibility of polymer modified binders.
- The 3% RPE modified mixture showed improved rutting resistance but reduced moisture resistance as the unmodified control mixture.
- Adding 3% RPE plus 1.2% RET significantly improved the rutting and moisture resistance of the unmodified control mixture. Note, however, that the improvement in moisture resistance was likely attributed to the inclusion of PPA as a catalyst for the RET additive used.
- Using RPE alone or RPE plus RET for asphalt modification did not have a significant impact on the mixture's resistance to intermediate-temperature fatigue cracking, thermal cracking, or reflective cracking.

Although this study demonstrated the feasibility and certain performance benefits of using RPE for asphalt modification, the scientific-based development of this concept is still at an

early stage and needs further research. For example, the above conclusions were made based on the testing of modified binders and mixtures consisting of one RPE sample and one base binder only; therefore, future research is needed to investigate the use of various additional types of RPE polymers and base binders for asphalt modification with known molecular compositions and structures. Furthermore, mechanistic-empirical pavement design analyses are recommended to determine the impact of RPE modified mixtures on the structural response and capacity of asphalt pavements under traffic. Research efforts on life-cycle cost analysis, life-cycle assessment, and recyclability evaluation are also needed to ensure that adding RPE has no negative impact on the cost-effectiveness, environmental impact, and recyclability of asphalt pavements or any unintended consequences on the health and safety of plant operators and construction crews. Finally, low-risk demonstration projects are recommended to identify the potential changes in the production and construction practices of RPE modified asphalt mixtures.

REFERENCES

Adams, J. J., Elwardany, M. D., Planche, J.-P., Boysen, R. B., and Rovani, J. (2019). Diagnostic Techniques for Various Asphalt Refining and Modification Methods. Energy & Fuels, 33(4), pp. 2680-2698.

American Chemistry Council. (2019). Guide to the Business of Chemistry. https://www.americanchemistry.com/GBC2019.pdf.

Anderson, M., Gayle, K., Douglas, H., and Philip, B. (2011). Evaluation of the Relationship between Asphalt Binder Properties and Non-Load Related Cracking. Journal of the Association of Asphalt Paving Technologists, Volume 80.

Appiah, J.K., Berko-Boateng, V.N., and Tagbor, T.A. (2017). Use of Waste Plastic Materials for Road Construction in Ghana. Case Studies in Construction Materials, Volume 6, pp. 1-7.

Bajpai, R., Khan, M.A., Sami, O.B., Yadav, P.K., and Srivastava, P.K. (2017). A Study on the Plastic Waste Treatment Methods for Road Construction. International Journal of Advance Research, Ideas and Innovations in Technology. Volume 3, Issue 6, ISSN: 2454-132X.

Baumgaertel, M., and Winter, H. H. (1989). Determination of discrete relaxation and retardation time spectra from dynamic mechanical data. Rheologica Acta, 28(6), 511-519.

Boysen, R. B. (2015). Adaptation of Existing Analytical Scale Size Exclusion Chromatography Methods. Technical White Paper FP22.

Boysen, R. B., and Schabron, J. F. (2013). The automated asphaltene determinator coupled with saturates, aromatics, resins separation for petroleum residua characterization. Energy & Fuels. 27, pp. 4654-4661.

Brown, H., Dubois, C.J., and Serrat, C. (2019). Elvaloy® RET and Post-Consumer Recycled Resins for Performance Graded Asphalts. Plastics Industry Association NEMO Meeting, Washington, D.C.

Central Pollution Control Board (CPCB). (2008). Performance Evaluation of Polymer Coated Bitumen Built Roads. PROBES/122/2008-2009.

Claudy, P. M., Letoffe, J. M., Rondelez, F., Germanaud, L., King, G., and Planche, J.-P. (1992). A new interpretation of time-dependent physical hardening in asphalt based on DSC and optical thermoanalysis. In ACS Symposium on Chemistry and Characterization of Asphalts, Washington, D.C.

Cronin, K. Email Correspondence titled “DSC Evaluation_RPE 1-4.” Received on June 27, 2019.

Elwardany, M. D., King, G., Planche, J.-P., Rodezno, C., Christensen, D., Fertig III, R. S., Kuhn, K. T., and Bhuiyan, F. H. (2019). Internal Restraint Damage Mechanism for Age-Induced Pavement Surface Distresses: Block Cracking and Raveling. Journal of the Association of Asphalt Paving Technologists (In press).

Environmental Protection Agency (EPA). (2018). How Do I Recycle? Common Recyclables. https://www.epa.gov/recycle/how-doi-recycle-common-recyclables, accessed on July 10, 2019.

Gawande, A., Zamre, G.S., Renge, V.C., Bharsakale, G.R., and Tayde, S. (2012). Utilization of Waste Plastic in Asphalting of Roads. Scientific Reviews & Chemical Communications, Volume 2(2), pp. 147-157.

Georgia Department of Transportation. (2013). Standard Specifications Construction of Transportation Systems.

Hintz, C., Velasquez, R., Johnson, C., and Bahia, C. (2011). Modification and Validation of the Linear Amplitude Sweep Test for Binder Fatigue Specification. Journal of the Transportation Research Board. Transportation Research Board, National Academies of Sciences, Washington, D.C., pp. 96-106.

Ho, S., Church, R., Klassen, K., Law, B., MacLeod, D., and Zanzotto, L. (2006). Study of Recycled Polyethylene Materials as Asphalt Modifiers. Canadian Journal of Civil Engineering, Volume 33, pp. 968-981.

Indian Roads Congress. (2013). Guidelines for the Use of Waste Plastics in Hot Bituminous Mixes (Dry Mixes) in Wearing Courses. IRC:SP:98-2013.

International Union of Laboratories and Experts in Construction Materials, Systems and Structures (RILEM). (2012). Proposal for a pre-normative FTIR method. TC SIB – TG5 – Recycling, September.

Jennings, P. W., Pribanic, P. W., Campbell, W., Dawson, K., Shane, S., and Taylor, R. (1980). High pressure liquid chromatography as a method of measuring asphalt composition (No. FHWA-MT-79-30 Final Rpt.).

Kim, Y., Lee, H.J., Little, D.N., and Kim, Y.R. (2006). A Simple Testing Method to Evaluate Fatigue Fracture and Damage Performance of Asphalt Mixtures. Journal of Association of Asphalt Paving Technologists, Vol. 75, pp. 755-788.

Liao, L., Li, H., and Wang, G. (2006). Research of Mixed-Waste Plastics from Urban Waste as Road Bitumen Modifier. China Resources Comprehensive Utilization, Volume 24, No. 9, pp. 28-32.

Liu, M., Chaffin, J. M., Davison, R. R., Glover, C. J., and Bullin, J. A. (1998). Changes in Corbett fraction composition during oxidation of asphalt fractions. Transportation research record, 1638(1), 40-46.

MacRebur, The Plastic Road Company. “It’s the end for the road for waste plastics.” https://www.macrebur.com/, accessed on July 21, 2019.

Moraes, R., Velasquez, R., and Bahia, H. U. (2011). Measuring the effect of moisture on asphalt–aggregate bond with the bitumen bond strength test. Transportation Research Record, 2209(1), 70-81.

National Center for Asphalt Technology (NCAT). (2019). Discussion on the Use of Recycled Plastics in Asphalt.

Panabaker, H. (2007). DuPont Innovative Asphalt Modifiers: How to save money with Elvaloy® RET and EntiraTM Bond asphalt modifiers. Southeast Asphalt User/Producer Group (SEAUPG) Annual Meeting, San Antonio, Texas.

Petersen, J. C. (2009). A review of the fundamentals of asphalt oxidation: chemical, physicochemical, physical property, and durability relationships. Transportation Research Circular E-C140.

Planche, J.-P., Elwardany, M. D., and Adams, J. J. (2018). Chemo-mechanical Characterization of Bitumen Binders with the Same Continuous PG–Grade. In RILEM 252-CMB-Symposium on Chemo Mechanical Characterization of Bituminous Materials (pp. 77-83). Springer, Cham.

Rad, F. Y., Elwardany, M. D., Castorena, C., and Kim, Y. R. (2017). Investigation of proper long-term laboratory aging temperature for performance testing of asphalt concrete. Construction and Building Materials, 147, pp. 616-629.

Robertson, R. E. (2000). Chemical properties of asphalts and their effects on pavement performance (No. 499). Transportation Research Board, National Research Council.

Rowe, G.M. (2011). Prepared Discussion for the AAPT Paper by Anderson et al.: Evaluation of the Relationship between Asphalt Binder Properties and Non-Load Related Cracking. Journal of the Association of Asphalt Paving Technologists, Vol. 80, pp. 649-662.

Ruan, Y., Davison, R. R., and Glover, C. J. (2003). Oxidation and viscosity hardening of polymer-modified asphalts. Energy & fuels, 17(4), 991-998.

Silva, H., and Oliveira, J., and Fernandes, S. (2013). Incorporation of Waste Plastic in Asphalt Binders to Improve Their Performance in the Pavement. International Journal of Pavement Research and Technology, Volume 6(4), pp. 457-464.

Tran, N, Yin, F., Leiva, F., Huber, G., and Pine, B. (2019). Adjustments to the Superpave Volumetric Mixture Design Procedure for Selecting Optimum Asphalt Content. Project NCHRP 20-07/Task 412.

Turner, T. F., and Branthaver, J. F. (1997). DSC studies of asphalt and asphalt components. In Asphalt Science and Technology, Usmani, A. M., Ed. Marcel Dekker Inc.: New York, NY; pp. 59-101.

West, R., Rodezno, C., Leiva, F., and Yin, F. (2018). Development of a framework for balanced mix design. Project NCHRP 20-07/Task 406.

White, G., and Reid, G. (2018). Recycled Waste Plastics for Extending and Modifying Asphalt Binders. Paper presented at the 8th Symposium on Pavement Surface Characteristics: SURF 2018 – Vehicle to Road Connectivity, Brisbane, Queensland.

Yang, X., and Liu, K. (2010). Reflections on Waste Plastic Modified Asphalt Research. Journal of Tibet University, Volume 25, No. 1, pp. 68-75.

Yin, F., Arambula, E., Lytton, R., Martin, A. E., and Cucalon, L. G. (2014). Novel method for moisture susceptibility and rutting evaluation using Hamburg wheel tracking test. Transportation Research Record, 2446(1), 1-7.

Zhou, F., S. Im, L. Sun, and T. Scullion. Development of an IDEAL Cracking Test for Asphalt Mix Design and QC/QA. *Road Materials and Pavement Design*, Vol. 18, pp. 405-427, 2017.